Chem Soc Rev

# Stimuli-responsive nanogel composites and their application in nanomedicine



| | |
|---|---|
| Journal: | *Chemical Society Reviews* |
| Manuscript ID: | CS-SYN-03-2015-000199.R2 |
| Article Type: | Review Article |
| Date Submitted by the Author: | 07-May-2015 |




| | |
|---|---|
| Complete List of Authors: | Molina, Maria; Freie Universität Berlin,<br>Asadian-Birjand, Mazdak; Freie Universität Berlin,<br>Balach, Juan; Institute for Complex Materials, Leibniz-Institute for Solid State and Materials Research Dresden,<br>Bergueiro, Julian; Freie Universität Berlin,<br>Miceli, Enrico; Freie Universität Berlin,<br>Calderon, Marcelo; Freie Universität Berlin, |

# Stimuli-responsive nanogel composites and their application in nanomedicine

Maria Molina[1], Mazdak Asadian-Birjand[1], Juan Balach[3], Julian Bergueiro[1], Enrico Miceli[1,2], and Marcelo Calderón[1,2,*]

[1] Freie Universität Berlin, Institute of Chemistry and Biochemistry, Takustr. 3, 14195 Berlin, Germany

[2] Helmholtz Virtuelles Institut – Multifunctional Biomaterials for Medicine, Helmholtz-Zentrum Geesthacht, Teltow, Germany

[3] Institute for Complex Materials, Leibniz-Institute for Solid State and Materials Research Dresden, Helmholtzstr. 20, D-01069 Dresden, Germany

* Corresponding author: Prof. Dr. Marcelo Calderón, Freie Universität Berlin, Institute for Chemistry and Biochemistry, Takustr. 3, 14195 Berlin, Germany, phone: +49-30-83859368, fax: +49-30-838-459368, e-mail: marcelo.calderon@fu-berlin.de

## Article outline

**Abstract**

Nanogels are nanosized crosslinked polymer networks capable of absorbing large quantities of water. Specifically, smart nanogels are interesting because of their ability to respond to biomedically relevant changes like pH, temperature, etc. In the last few decades, hybrid nanogels or composites have been developed to overcome the ever increasing demand for new materials in this field. In this context, a hybrid refers to nanogels combined with different polymers and/or with nanoparticles such as plasmonic, magnetic, and carbonaceous nanoparticles, among others. Multifunctional hybrid nanogels are focused nowadays on nanomedicine, not only as drug carriers but also as imaging and theranostic agents. In this review, we will describe nanogels, particularly in the form of composites or hybrids applied in nanomedicine.

**Keywords**

Composites, core-shell, hybrid, imaging, interpenetrating networks, nanogel, nanomedicine, plasmonic nanoparticles, stimuli-responsive, theranostic

**Abbreviations**

| | |
|---|---|
| AA | acrylic acid |
| AEMA | 2-amino-ethyl methacrylamide hydrochloride |
| AFM | atomic force microscopy |
| AgNPs | silver nanoparticles |
| AMF | alternating magnetic field |
| APBA | 3-acrylamidophenylboronic acid |
| ARS | alizarin red S |
| ASGP-R | asialoglycoprotein receptor |
| ATRP | atom-transfer radical polymerization |
| Au@NGs | gold hybrid nanogels |
| AuNPs | gold nanoparticle |
| BAP | poly(1-(2-aminoethyl)piperazine-co-N,N'-bis(acryloyl)cystamine) |
| BCA | bicinchoninic acid |
| bPEI | branched polyethyleneimines |
| BSA | bovine serum albumin |
| Ce6 | chlorin e6 |
| CHI | chitosan |
| CHP | cholesterol-bearing pullulan |
| $CHPNH_2$ | amino-modified CHP |
| CNTs | carbon nanotubes |
| Cy5.5 | Cyanine5.5 |
| DDOPBA | 4-(1,6-dioxo-2,5-diaza-7-oxamyl)phenylboronic acid |
| Dex | dextran |

| | |
|---|---|
| DMAP | 4-dimethylaminopyridine |
| DMSO | dimethylsulfoxide |
| DOTA | 1,4,7,10-tetraazacyclododecane-1,4,7,10-tetraacetic acid |
| DOX | doxorubicin |
| DTPA | diethylenetriaminepentaacetic acid |
| DTT | dithiothreitol |
| EDC | 1-Ethyl-3-(3-dimethylaminopropyl)carbodiimide |
| EGDMA | ethylene glycol dimethacrylate |
| FDA | food and drug administration |
| FITC | fluorescein isothiocyanate |
| FPBA | 2-acrylamidomethyl-5-fluorophenylboronic acid |
| FRET | fluorescence resonance energy transfer |
| 5-FU | 5-fluorouracil |
| Gal | galactosylated |
| Gd | gadolinium |
| HPC | hydroxipropylcellulose |
| hMSCs | human mesenchymal stem cells |
| HUVECs | human umbilical vascular endothelial cells |
| IB | ibuprofen |
| INH | isoniazid |
| IPN | interpenetrating polymer network |
| iRGD | tumor targeting peptides (CRGDRCPDC)-SH) |
| i.v. | intravenous |
| LCST | lower critical solution temperature |
| LRP1 | lipoprotein receptor-related protein 1 |
| MBAAm | N,N′-methylenebisacrylamide |
| MEA | methacryloylethyl acrylate |
| MeODEGM | methoxydiethylene glycol methacrylate |
| mMePEG | monomethoxy-PEG |

| | |
|---|---|
| MePEGA | methoxyl-PEG methacrylate |
| $MnFe_2O_4$ | manganese iron oxide |
| MRI | magnetic resonance imaging |
| MTs | magneto-transducers |
| NaAlg | sodium alginate |
| NDs | nanodiamonds |
| NHS | N-hydroxysulfosuccinimide |
| NIPAm | N-isopropylacrylamide |
| NIPMAm | N-isopropylmethacrylamide |
| NIR | near infrared |
| ODN | oligonucleotides |
| PAA | polyacrylic acid |
| PAAm | polyacrylamide |
| Pasp | poly(aspartic acid) |
| PBA | phenylboronic acid |
| PBS | phosphate buffered saline |
| PDT | photodynamic therapy |
| PEAMA | poly-[2-(N, N- diethylamino) ethyl methacrylate] |
| PEG | polyethilenglycol |
| PEG-d | polyethylene glycol-diacrylate |
| PEOMA | poly(ethylene glycol) methyl ether methacrylate |
| γ-PGA | poly(γ-glutamic acid) |
| PLL | poly(L-lysine) |
| PMAA | poly(methacrylic acid) |
| PNIPAm | poly(N-isopropylacrylamide) |
| PNIPMAm | poly(N-isopropylmethacrylamide) |
| POEG | poly(oligo ethylene glycol) |
| PPE | polyphosphoester |
| PSI | poly(succinimide) |

| | |
|---|---|
| PSNPs | porous silica nanoparticles |
| PT | photothermal transductor |
| PTT | photothermal therapy |
| PVA | polyvinyl alcohol |
| P(VA-b-VCL) | poly(vinyl alcohol-*b*-*N*-vinylcaprolactam) |
| p(VPBA-c-DMAEA) | poly(4-vinylphenylboronic acid-*co*-2-(dimethylamino)ethyl acrylate) |
| QDs | quantum dots |
| QD@NGs | quantum dot hybrid nanogels |
| QT | pentaerythritol tetra(3-mercaptopropionate) |
| RAFT | reversible addition−fragmentation chain-transfer polymerization |
| RES | reticuloendothelial system |
| RF | radiofrequency |
| rGO | reduced graphene oxide |
| RHB | Rhodamine B |
| SANS | small-angle neutron scattering |
| SAXS | small-angle X-ray scattering |
| SEM | scanning electron microscopy |
| SERS | surface-enhanced raman scattering |
| sIPN | semi interpenetrating polymer network |
| siRNA | short interfering RNA (ribonucleic acid) |
| SPIONs | super paramagnetic iron nanoparticles |
| TEGDP | 3,6-dioxaoctan-1,8-diyl bis(ethylene phosphate) |
| TEM | transmission electron microscopy |
| TMZ | temozolomide |
| UCST | upper critical solution temperature |
| YSA | 12 amino acid peptide (YSAYPDSVPMMS) |

## 1. Introduction

Nanogels are nanosized hydrogel particles that combine the properties of both hydrogels and nanomaterials.[1] Like hydrogels, they show high water content, tunable chemical and physical structures, good mechanical properties, and biocompatibility.[2] The nanoscale mainly provides a large surface area for bioconjugation, long time of circulation in blood, and tunable size from nanometers to micrometers with the possibility of being actively or passively targeted to the desired site of action, e.g., tumor sites.[3] The sum of these properties plus the presence of an interior network for the encapsulation of biomolecules make nanogels ideal candidates for their application in nanomedicine.[4, 5] Nanomedicine is the application of nanotechnologies to the medical field as drug delivery systems, imaging and sensing agents, theranostic materials, among others. Smart nanogels have attracted much attention for their application in medicine due to their capacity to respond to divers medically relevant stimuli[6] like pH,[7] temperature,[8-11] ionic force,[12] redox environment,[13] etc., by changing their volume, refractive index, and hydrophilicity–hydrophobicity.[14]

In recent years, the development of advanced or hybrid nanogels with multifunctionality and novel properties has been of interest in many research fields ranging from materials science to nanomedicine.[15, 16] Hybrid nanogels can be classified based on their different properties. For the purpose of this review, we divided the hybrid nanogels in two categories: nanomaterial-nanogels and polymer-nanogels composites and we use @ in the nomenclature of the nanomaterial-nanogel composites meaning that the new component is hybridized with the nanogel. Nanomaterial-nanogels composites have also been synthesized by incorporation of nanosized materials such as plasmonic,[17, 18] magnetic,[19-21] and carbonaceous materials nanoparticles,[22] like carbon nanotubes,[23, 24] graphene,[25] and fullerenes.[26] These materials are of great interest in nanomedicine due to their applicability for imaging,[27] guided therapy,[19] triggered drug release,[28] and hyperthermia,[29] among others. Furthermore, polymer-nanogels composites include

interpenetrated networks (IPNs) and core-shell particles. The advantage of hybridizing the nanogels with other polymers and not only copolymerizing them is that each component maintains its original properties. The core-shell strategy is especially useful for targeting therapy[30] while the interpenetration allows the development of multiresponsive nanogels[31] and the control of the release profile.[32] Several reviews about synthesis and characterization of nanogels have been published. [4, 33-36] In this review, we will focus on the description of different hybrid nanogels and their application in the nanomedicine field (Figure 1). In addition, it is hoped that this review will promote further design and development of new hybrid materials as well as deeper studies for shortening the path to their clinical application.

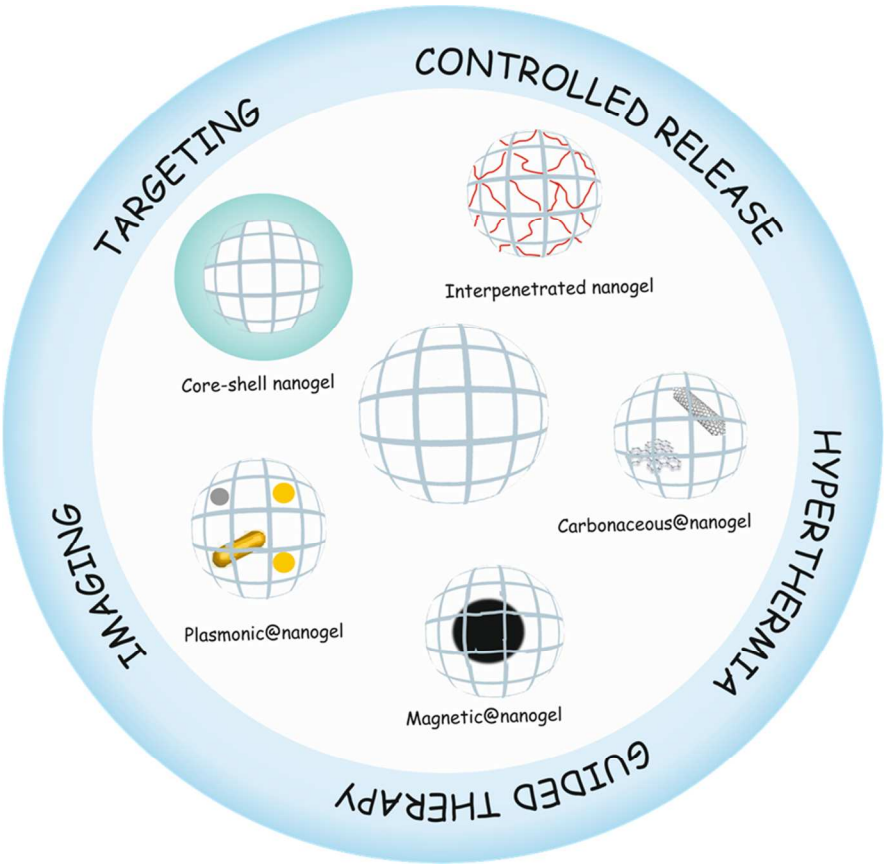


**Figure 1.** Hybrid nanogels and their application in nanomedicine.

## 2. Nanomaterial-nanogel composites

The possibility of combining properties of organic and inorganic components in one material widens their applications in different fields like materials science. However, the so-called hybrid inorganic–organic materials are not physical mixtures but intimately mixed systems. The resulting properties, such as nanostructure, degree of organization, etc., not only depend on their components' nature but also on the synergy between the components. These inorganic-organic composites can be classified according to the nature of the interactions between the components in: (a) class I systems where no covalent bonds are formed between the organic and inorganic components and only weak interactions are present such as hydrogen bonding, van der Waals, or electrostatic forces and (b) class II where strong chemical bonds such as covalent or Lewis acid-base bonds are present.[37, 38] Without any doubt, these new generations of hybrid materials will open up new possibilities for application in different areas of nanomedicine as, for example, optical sensing,[39] on demand drug delivery,[40] imaging,[41] and hyperthermia therapy.[19]

In this section different nanomaterial-nanogels and their application in nanomedicine will be described, including plasmonic@, magnetic@, carbonaceous material@nanogels.

### 2.1. Plasmonic@nanogels

Photothermal therapy (PTT) and photodynamic therapy (PDT) are currently the most promising techniques for treating cancer.[42] This is because of the possibility of engineering devices in the nanometric scale that present photothermal transductors (PTs) with absorption in the biological window. Near infrared irradiation (NIR) is known as biological window since it is hardly absorbed by water and blood cells and can penetrate deeply into the body. PDT is based on PTs that can use NIR light to produce reactive oxygen species which induces tissue destruction. On the other hand, PTT makes use of specific PTs that

can effectively transform NIR light into local heat, surpassing the traditional hyperthermia methods such as hot-water bath or heated blood perfusion.[43] Nanogels composed of PTs and different polymers are ideal nanodevices for PTT because of their controlled size and architecture, biocompatibility, degradation ability, physical properties, accumulation in tumors, loading capacity, and post synthetic modification.[14] Moreover state-of-the-art drug delivery systems have emerged that make use of thermoresponsive polymers that can swell or shrink with the temperature in combination with PTs.[44] The local heat produced by PTs upon exposure to specific radiation causes the transition of the thermoresposive polymer and expels the drug retained into it.

Gold nanoclusters have proven to be useful agents for PTT after they were shown to have an absorption in the NIR region four times higher than conventional photo-absorbing dyes. More specifically, gold nanorods (AuNRs) have been extensively explored due to their aspect ratio that enables efficient NIR light absorption. Photoexcitation of metal nanostructures causes local heating which is useful for PTT. Magnetic nanoparticles (Section 2.2) can also generate local heating when they are exposed to an alternating magnetic field (AMF) acting as magnetic transductors.[45, 46] Some of the most employed PTs like gold nanoparticles (AuNPs) as well as magnetic and silver nanoparticles (AgNPs) also have the advantage of acting as a contrast agent for bioimaging. All these properties favor the use of plasmonic hybrid nanogels as theranostic agents in chemo- and thermotherapy as well as *in vitro* or *in vivo* imaging.[47] Table 1 summarizes recent examples that are discussed on the following sections and highlight the potential of the plasmonic NPs@nanogels as theranostic agents.

**Table 1.** Plasmonic hybrid nanogels as theranostic agents.

| Plasmonic | Polymer | Stimuli | Application | Theranostic | Ref. |
|---|---|---|---|---|---|

| NPs | | | | Agent | |
|---|---|---|---|---|---|
| AuNPs | PEG | NIR Light | Imaging (internalization) | AuNPs | 55 |
| AuNPs | PEAMA-PEG | Caspase-3 | Imaging (FRET, internalization) | FITC | 56 |
| AuNPs | PAA | NIR Light | Imaging (biodistribution) | Au Nanoclusters | 57 |
| AuNPs | PEAMA-PEG | NIR Light | Hyperthermia | AuNPs | 58 |
| AuNRs | Pluoronic | NIR Light | PTT and PDT | Ce6 | 59 |
| AuNPs | Polyamine | X-rays | RF Hyperthermia | - | 60 |
| AuNPs-$MnO_2$NRs | Chitin | Radio Frequency | RF Hyperthermia | AuNPs-$MnO_2$NRs | 61 |
| AuNPs | PNIPAm-IPN | Temperature | Hyperthermia – Drug delivery | 5-FU | 62 |
| Au nanoclusters | P(NIPAm-co-AA) | Temperature | Hyperthermia – Drug delivery | DOX | 63 |
| AuNRs | PNIPAm | NIR Light-Temperature | Hyperthermia – Drug delivery | - | 64 |
| AuNRs | PNIPAm | NIR Light-Temperature | Hyperthermia – Drug delivery | DOX | 65 |
| Au-AgNRs | PAA-Aptamers | NIR Light | Hyperthermia – Drug delivery | DOX | 66 |
| Au-AgNPs | PS-PEG | NIR Light | Hyperthermia – Drug delivery | Curcumin | 67 |
| AgNPs | P(NIPAm-co-AA) | pH | Imaging – Drug delivery | Dipyridamole | 69 |
| AgNPs | P(NIPAm-co-DMAEA) | pH | Imaging – Drug delivery | Insulin | 70 |

### 2.1.1. Gold@nanogels

AuNPs of different shapes internalized in nanogels have been widely explored. The

synthesis of these gold nanocomposites can be mainly achieved by two approaches: (a) pre-synthesis of plasmonic nanoparticles and posterior growing of the nanogel or internalization into it,[48-51] or (b) in situ generation of nanoparticles inside the nanogel.[52-54]

Gold hybrid nanogels (Au@NGs) have been reported as relevant bioimaging devices. Siegwart et al.[55] described uniformly crosslinked poly(ethylene glycol) (PEG) based nanogels synthesized by atom transfer radical polymerization (ATRP) into which AuNPs were entrapped. Cell uptake and internalization of these nanodevices have been studied in human umbilical vascular endothelial cells (HUVECs) and human mesenchymal stem cells (hMSCs) validating an endocytosis mechanism. A similar approach by Oishi et al.[56] made use of the fluorescence resonance energy transfer (FRET) between AuNPs and fluorescein isothiocyanate (FITC) in a PEGylated Au@NG. A caspase-3-responsive system was designed to monitor the cancer response to therapy. A pronounced fluorescence was observed when the activated caspase-3 in apoptotic cells cleaved the Asp-Glu-Val-Asp peptide that resulted in a release of the FITC and dequenching of its fluorescence. The biodistribution of poly(acrylic acid) (PAA) nanogels with AuNPs formed *in situ* was recently studied on H22 tumor-bearing mice.[57] Gels mainly accumulated in the liver and spleen because of their capture by phagocytic cells of the reticuloendothelial system (RES) of these organs.

Au@NGs are not only interesting for bioimaging by employing the optical properties of the gold. In the last decade, the use of non spherical AuNPs as PTs in Au@NGs enabled its advantageous application in PDT and PTT. PEGylated poly-[2-(N, N- diethylamino) ethyl methacrylate] (PEAMA) core nanogels with AuNPs post-synthesized by reduction of Au(III) ions reported by Nakamura et al.[58] showed high biocompatibility and remarkable photothermal efficacy. PTT in response to 514.4 nm light was achieved in HeLa cells, killing only the cells in the laser area with low $IC_{50}$ values depending on the gold

concentration of the nanogel. One of the most relevant examples in this field is the PPT and PDT synergistic combination from Kim et al.[59] with Pluronic based nanogels loaded with AuNRs as PTT agent and chlorin e6 (Ce6) as photosensitizer. *In vitro* SCC7 cell line and *in vivo* SCC7 tumor bearing mice remarkably enhanced the combination of PTT and PDT. But even more interestingly, the tumor decreased in size when the PDT was applied before PTT. When PTT was applied first the combined therapy was not so effective as with just PTT. This comparative study therefore revealed a more convenient way to use of photo-therapies. The radiosensitizing potential of gold containing nanogels enhancing the biological effect of X-irradiation was studied with PEGylated polyamine nanogels containing AuNPs.[60] This report proved that these devices enhanced the cell radiosensitivity because of the induction of apoptosis and the inhibition of DNA double-strand break repair by Au@NG mediated endoplasmic reticulum stress. A combination of chitin nanogels with AuNPs and $MnO_2$ rods was also used for radiofrequency (RF) assisted hyperthermia.[61] Au@NGs showed better results in the ablation of T47D cancer cells than the bare nanogels.

Au@NGs formed by thermoresponsive polymers controlled by PTs were used as smart drug delivery systems in combination with hyperthermia. Thus, these nanogels are theranostic systems with drug delivery, hyperthermia, and bioimaging capabilities. Poly(*N*-isopropylacrylamide) (PNIPAm) is a thermoresponsive polymer with a lower critical solution temperature (LCST) of around 32 ºC which is suitable for medical applications. PNIPAm based nanogels were reported in combination with AuNPs in a core-shell fashion.[62] Au@PNIPAm nanogels were employed in cell imaging trespassing cellular barriers to enter the cytoplasm. 5-fluoroacyl (5-FU) served as model anticancer drug to test the viability of HeLa cells upon exposure to 515 nm laser. Cell death increased significantly in the drug loaded systems in comparison to non-loaded ones, which

demonstrated the higher therapeutic efficacy of the combined chemo-photothermal treatments. P(NIPAm-co-AA) nanogels with incorporated gold nanoclusters were employed as a doxorubicin (DOX) delivery system.[63] In this case, the dual thermo- and pH-responsive systems were decorated with tumor targeting peptides like (CRGDRCPDC)-SH (iRGD) that showed good results in HUVECs and extravascular tumor cells (B16). More convenient PTs like gold nanorods (AuNRs) were studied as building blocks in nanogel based drug delivery systems. Kawano et al.[64] proved that silica coated AuNR core-shell PNIPAm hybrid nanogel underwent phase transition and accumulated into NIR irradiated target sites. A similar system was used as a NIR guided DOX delivery system.[65] After NIR irradiation the accumulation in tumor post systemic administration was enhanced with almost a total tumor growth inhibition as well as lung metastasis (Figure 2).

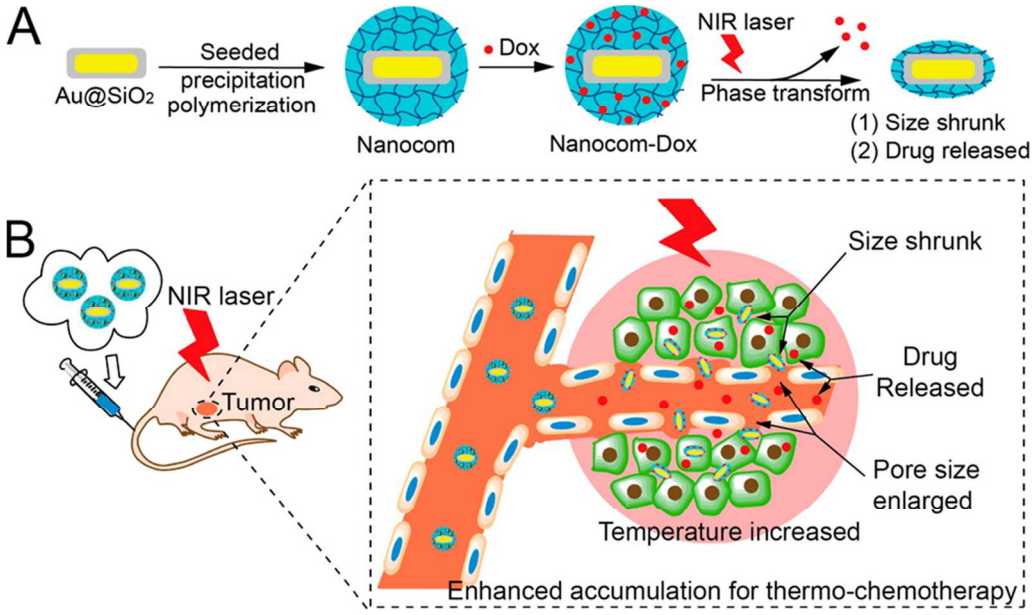


**Figure 2.** (A) Hybrid nanogel synthesis and (B) NIR laser induced targeted therapy using the hybrid nanogel. Reprinted with permission from Ref. 65. Copyright 2014 American Chemical Society.

Gold-silver nanorods (Ag-AuNRs), which can absorb NIR photons more efficiently than spherical gold and silver nanoparticles but combining their basic properties, were used as PTs in polyacrylamide based nanogels, crosslinked by complementary DNA strands. Nanogels were functionalized with DNA aptamers for specific tumor cells targeting.[66] DOX was loaded into DNA aptamers that responded upon local heating by NIR irradiation of the PT releasing the drug. Studies in CCRF-CEM cells and Ramos cell line as the control demonstrated low cytotoxicity of the nanogels as well as high specificity for tumor cells after NIR irradiation. Bimetallic gold-silver nanoparticles were also reported in core-shell polystyrene/PEG based nanogels.[67] Au-Ag@NGs were able to encapsulate drugs like curcumin that has pro-apoptotic effects. Upon NIR light exposure, the release of drug could be triggered by the outer PEG shell thermoresponsivity to local temperature increase. *In vitro* comparative study of these systems in B16F10 cells revealed an enhanced effect of chemo- and thermotherapies.

### 2.1.2. Silver@nanogels

AgNPs present interesting properties that encouraged various research groups to incorporate them into nanogel architectures.[68] AgNPs have well-known antimicrobial properties as well as optical properties for potential biodiagnostic imaging. In the core-shell Ag@NGs of P(NIPAm-co-AA) reported by Wu and Zhou[69] the AgNP core acted as an optical identification code for tumor cell imaging, while the P(NIPAm-co-AA) gel shell served as drug carrier with high loading capacity of dipyridamole as a model drug. Because of the pH response of the P(NIPAm-co-AA) shell, the physicochemical environment of the AgNPs changed. This alteration affected the optical properties of the core and also modified the mesh size of the gel. This phenomenon was used to regulate the drug release behavior in B16F10 cell line. A similar approach was done to deliver

insulin by employing a AgNP core and a pH-responsive nanogel shell of poly(4-vinylphenylboronic acid-*co*-2-(dimethylamino)ethyl acrylate) [p(VPBA-c-DMAEA)].[70]

### 2.2. Magnetic@nanogels

Within nanomaterial-nanogels composites, magnetic nanoparticles have attracted interest because of their application as PTs and in imaging. In the past, the most common methodology for preparing super paramagnetic iron nanoparticles (SPION)[71] was performed by reduction and coprecipitation of ferrous and ferric salts in aqueous media in the presence of stabilizers. This procedure has led to several commercial products like Feridex® (Ferumoxides),[72, 73] Resovist® (Ferucarbotran),[73-75] and Ferumoxtran-10® (Combidex).[73, 74, 76] As their biodistribution depended on their size and surface modification, much effort has been made in developing magnetic nanomaterials with increased colloidal stability under physiological conditions. Moreover, the research focus was on improving contrast properties while lowered cytotoxicity, maintained longer blood half-life, improved biocompatibility, and enhanced tissue/organ targeting ability as well as pharmaceutical efficacy due to surface functionalization.[77] Today, to accomplish the requirements for safer and more efficient nanostructure-based contrast agents, the developed materials have become more complex as nanoclusters,[78] polymersomes,[79, 80] nanocomposites,[81-88] and nanogels.[89-93] Considering the obtained impressive biodistributions and remarkable magnetic resonance imaging (MRI) properties, the following section presents recent developments of hybrid nanogels for magneto-transducers (MTs) and MRI.

**Table 2.** Characteristics of magnetic@nanogels and MRI contrast agents.

| Compound | Magnetic material | Matrix / coating | Relaxivity@ 1.5T [$mM^{-1}s^{-1}$] $r_1/r_2$ | Stimuli | Application | Ref. |
|---|---|---|---|---|---|---|
| Feridex® (ferumoxides) | $Fe_3O_4$ | Dextran | 24/98 | - | Commercial ($T_2$) MRI contrast agent | 73 |
| Resovist® (Ferucarbotran) | $Fe_3O_4$ | Carboxydextran | 25/151 | - | Commercial ($T_1$ & $T_2$) MRI contrast agent | 73,75 |
| Ferumoxtran-10® (Combidex) | $Fe_3O_4$ | Carboxydextran | 10/60 | - | Commercial ($T_2$) MRI contrast agent | 73,76 |
| $\gamma$-$Fe_2O_3$@P(VA-b-VCL) | $\gamma$-$Fe_2O_3$ | P(VA-b-VCL) | -/37 | Glucose, pH, temperature, AMF | Multiresponsive drug delivery system and $T_2$ contrast agent | 94 |
| SPION@AA-NIPAm-MEA-PEG | $Fe_3O_4$ | AA-NIPAm-MEA-PEG | -/265.5 | Temperature, pH, AMF | Multiresponsive drug delivery system and $T_2$ contrast agent | 95 |
| $MnFe_2O_4$@PGA-PLL(PEG) | $MnFe_2O_4$ | PGA-PLL(PEG) | -/382.6 | AMF | Intravenous (i.v.) injectable $T_2$ contrast agent for dual bio-imaging | 92 |
| SPION@NIPAm-AA-Cy5.5-Lf | $Fe_3O_4$ | PNIPAm-co-AA | -/142.7 | Temperature, pH, AMF | i.v. injectable $T_2$ contrast agent for dual bio- | 90 |

| | | | | | | |
|---|---|---|---|---|---|---|
| | | | | | imaging | |
| Magnevist® (Gd(III)–DTPA) | Gd(III) | DTPA chelate | 4.7/9.6 | - | Commercial ($T_1$) MRI contrast agent | 99 |
| Gd@nanogel (surface coordinated) | Gd(III) | PEOMA, AEMA, EGDMA, DTPA | 17.5/- | AMF | i.v. injectable $T_1$ contrast agent for bio-imaging | 91 |
| Gd@nanogel (incorporated) | Gd(III) | bPEI (core), mMePEG (shell), Cy5.5 | 2.1/82.6 | AMF | i.v. injectable $T_2$ contrast agent for dual bio-imaging | 89 |
| Gd@nanogel (incorporated) | Gd(III) | PAA DOTA-chelate-crosslinker | 17.6/- | AMF | Potential $T_1$ contrast agent | 101 |

MTs like SPIONs were used as an alternative to PTs. As an example, $\gamma$-$Fe_2O_3$ magnetic NPs were internalized in poly(vinyl alcohol-*b*-*N*-vinylcaprolactam) [P(VA-b-VCL)] based nanogels for glucose-, pH-, and thermo-responsive release of DOX.[94] AMF induced heating could be generated because of the superparamagnetic properties of the SPIONs that accelerated the drug release performance of the system. Chiang et al. also reported the use of AMFs to enhance drug release[95] from hybrid hollow nanogels formed with PEG, AA, PNIPAm, and crosslinked by photo-initiated polymerization of 2-methacryloylethyl acrylate (MEA). The DOX loaded nanogels exhibited accelerated drug release in response to pH reduction and hyperthermia. Magnetic properties of the nanogel were employed not only for AMF therapy but, moreover, for guided transport toward the target and MIR.

Enhanced *in vitro* cytotoxicity against HeLa cells in comparison with free DOX demonstrated the great potential of the multimodal theranostic system capable of combining hyperthermia and chemotherapy (Figure 3).

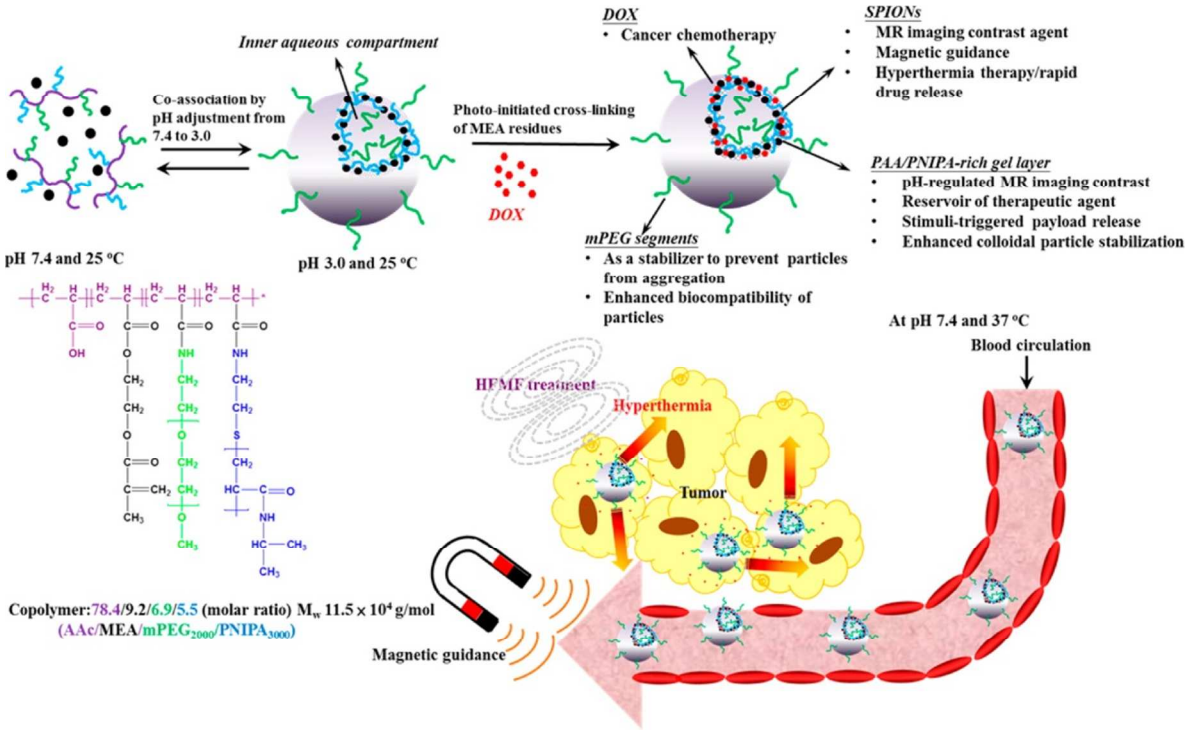


**Figure 3.** DOX-loaded hybrid nanogels as multifunctional anticancer theranostic system. Reprinted with permission from Ref. 95. Copyright 2013 American Chemical Society.

MRI is a widely known noninvasive imaging technique that achieves notable high spatial and temporal resolution. It displays contrast by visualizing changes in water proton density and longitudinal ($T_1$) or transversal ($T_2$/$T_2$*) relaxation times of protons in normal and diseased tissues.[96] Since their first use as MRI contrast agents 30 years ago,[97] iron oxide nanoparticles have gained much attention because of their ability to dramatically shorten $T_2$/$T_2$* relaxation times and therefore produce a decreased signal intensity in $T_2$/$T_2$* weighted MR images. With their specific accumulation in liver, spleen, and bone marrow,

their high magnetization, increment contrast visualization more than conventional paramagnetic $T_1$ contrast agents, they have exerted a high impact on the field of molecular and bio-imaging.[98]

In spite of a multi-modal approach for magnetic nanogels, Kim et al.[92] developed a self-fluorescent, and at the same time, high-relaxivity $T_2$-weighted MRI contrast agent for both MRI and optical bio-imaging. The formulation was achieved by electrostatic assembly and crosslinking of poly(γ-glutamic acid) (γ-PGA) coated manganese iron oxide ($MnFe_2O_4$) nanoparticles with the positively charged polyelectrolyte poly(l-lysine) (PLL). During the ionic gelation process, glutaraldehyde was added to the mixture which provided both structural integrity in the nanogel and involved formation of a self-fluorescent chemical bond. These fluorescent bonds were generated by the crosslinking of PLL with the glutaraldehyde monomer. Finally, PEG was conjugated to the surfaces of the $MnFe_2O_4$@PGA-PLL(PEG) nanogels. The $r_2$ value, which is known as relaxivity, is the reciprocal of the T2 relaxation time per unit concentration of metal ions. This value was 382.6 (Fe+Mn) $mM^{-1}$ $s^{-1}$ for the nanogel, two folds higher as compared to the $r_2$ of conventional SPION contrast agents as Feridex® and Resovist® (Table 2). The remarkable increment in $r_2$ resulted from the synergistic magnetism of the multicore $MnFe_2O_4$ nanoparticle satellites that were embedded in the nanogels. Moreover, $MnFe_2O_4$@PGA-PLL(PEG) nanogels also generated a strong fluorescence signal indicating that these compounds can be used as an imaging technique in living tissues. *In vivo* NIR fluorescence and MRI of lymph node in a mice model highlighted the nanogel's passive targeting ability to successfully migrate from injection site to the lymph node. The results suggest that after the incorporation of therapeutic moieties these systems could be a potent tool in theranostic technology.

A similar approach in multi-modality was performed by Jiang et al.[90] when engineering pH and temperature sensitive magnetic nanogels conjugated with Cyanine 5.5-labeled lactoferrin (Cy5.5-Lf) for MRI and fluorescence imaging of glioma in rats (Figure 4). In this study, citric acid coated SPIONs were incorporated in nanogels by free radical dispersion polymerization with NIPAm and AA as environmental sensitive monomers, and N,N'-methylenebisacrylamide (MBAAm) as the crosslinker. After polymerization, the surface coating was achieved by peptide coupling chemistry mediated conjugation of Cy5.5-Lf providing both a dual imaging modality and a targeting ligand for specific targeting of lipoprotein receptor-related protein 1 (LRP1) expressing cells. The obtained nanogels showed $r_2$ value of 142.7 $mM^{-1}$ $s^{-1}$, similar to the one of Resovist®, and revealed pH and temperature sensitiveness for enhanced targeting modalities. In fact, SPION@NIPAm-AA-Cy5.5-Lf nanogels were hydrophilic and swollen under physiological conditions (pH 7.4, 37 °C), which could prolong the blood circulation time, but became hydrophobic and shrunken under acidic environment of tumor tissues (pH 6.8, 37 °C). As a result, they could be more easily accumulated in tumor tissue and internalized by tumor cells. Cellular uptake studies on both rat C6 glioma cells (high LRP1 expression) and human umbilical vein endothelial (ECV 304) cells (no LRP1 expression), interestingly revealed that the cellular uptake of both SPION@NIPAm-AA-Cy5.5-Lf nanogels and NIPAm-AA nanogels at pH 6.8 was significant higher than that at pH 7.4. These results suggested that the nanogels' hydrophilic / hydrophobic transition and their change in size would increase their cellular uptake, as well as improve their internalizations in malignant tissues. SPION@NIPAm-AA-Cy5.5-Lf nanogels were applied *in vivo* and their imaging properties were evaluated on rats bearing C6 glioma both with MRI and fluorescence imaging technique. As a result, histopathological analyses obtained significant targeting ability for SPION@NIPAm-AA-Cy5.5-Lf nanogels on gliomas both *in vitro* and *in vivo*.

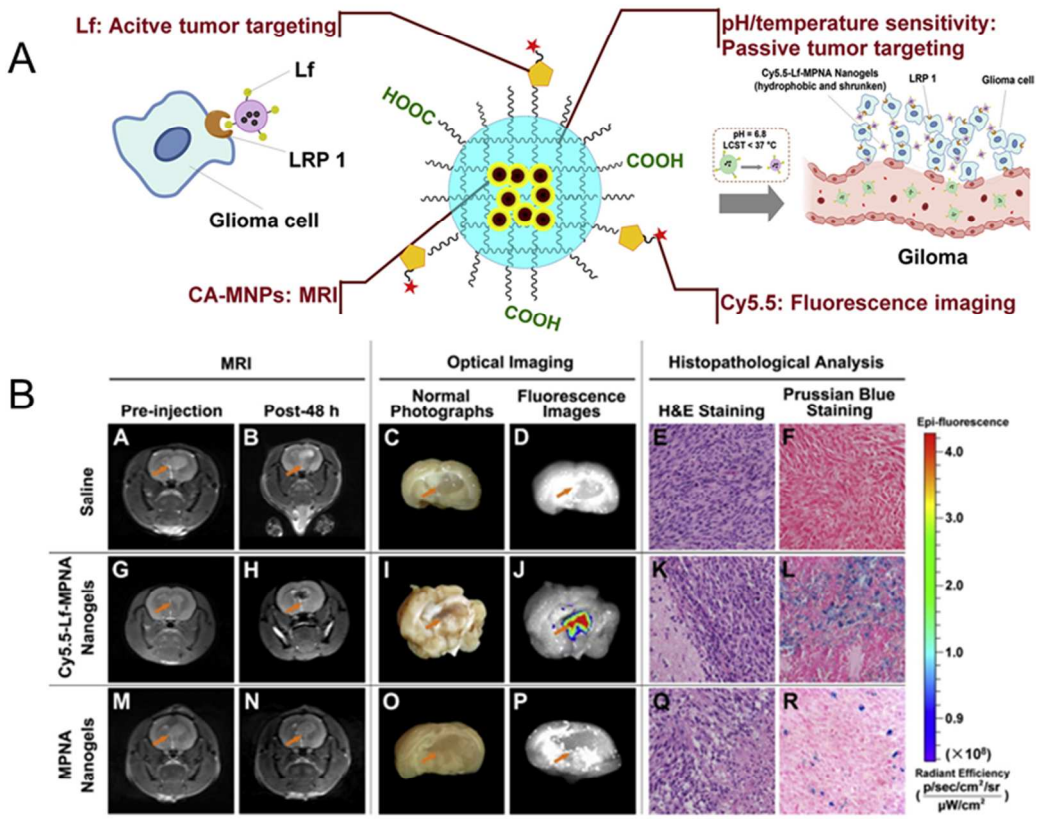


**Figure 4.** (A) Schematic representation of SPION@NIPAm-AA-Cy5.5-Lf. (B) *In vivo* studies: MRI, optical imaging, and histophatological analysis of of rats bearing gliomas treated with saline as a control (upper row), SPION@NIPAm-AA-Cy5.5-Lf nanogels (middle row), and NIPAm-AA nanogels (lower row), respectively. Reprinted from Ref. 90 . Copyright (2013), with permission from Elsevier.

Even though such impressive investigations have been performed as mentioned above, SPIONs generally provide some conceptual disadvantages that may limit their advanced clinical use. On the one hand, $T_2$ contrasting agents are negative contrast agents that can lead to signal-decreasing effects. As a result, the obtained dark signals could be mistaken for other pathogenic conditions leading to images of lower contrast than $T_1$ contrasted images. On the other hand, a high $T_2$ contrast agent susceptibility might induce distortion

of the magnetic field on the neighboring tissues. This background distortion is the so-called susceptibility artifact, which can yield obscure images and ruin the background around the malignant tissue.[71, 96] Therefore, the most used clinical contrast agents are based on gadolinium complex $T_1$ agents such as Magnevist (Table 2). Since these commercial available $T_1$ agents provide a relatively short blood half-life and low contrast efficiency due to low relaxivity values,[99] the scientific community aimed to improve their clinical impact through nanotechnology.[77, 96] As an example, Soleimani et al.[91] recently developed small nanogels (~10 nm diameter) based on poly(ethylene glycol) methyl ether methacrylate (PEOMA) and N-(2 aminoethyl) methacrylamide hydrochloride (AEMA) as monomers, and ethylene glycol dimethacrylate (EGDMA) as crosslinker. The nanogel's surface was decorated with an iso-thiocyanate derivative of the clinically used chelate diethylenetriaminepentaacetic acid (DTPA) which was able to complex gadolinium (Gd(III)) ions out of an aqueous $GdCl_3$ / nanogel solution mixture. Compared with the clinical agent Magnevist® (Gd(III)–DTPA),[99] the Gd(III) coated nanogels provided a 4 fold enhancement in $r_1$ relaxivity (Table 2). The higher contrast at the same dose in $T_1$ weighted MR images of C.B.-17 SCID mice bearing MDA-MB-231 tumors was achieved for nanogels indicated an increased accumulation in the tumor due to enhanced circulation in the vasculature.

A similar observation has been made in another approach incorporating Gd(III) ions into a nanogel matrix by Lim et al.[89] Here, $GdCl_3$ was coordinated to branched polyethyleneimines (bPEI) through an inverse miniemulsion technique of Tween 80 stabilized water droplets in cyclohexane. The obtained physically crosslinked nanogels (160 nm in diameter) were subsequently modified with a Cy5.5 dye to yield nanogels with a dual-imaging modality. Moreover, the labeled nanogels were coated with linear poly(ethylene glycol) N-hydroxy succinimide (PEG-NHS), as a stealth agent in order to increase the blood circulation time. As expected, low cytotoxicity and high deformability in

terms of Young's modulus were obtained, which subsequently led to minimal filtration by the RES and therefore increment passive accumulation in the tumor of a SCC7 tumor bearing mouse. Interestingly, no enhanced $T_1$-weighted MRI contrast was observed ($r_1$ = 2.1 $mM^{-1}s^{-1}$), but the remarkable $r_2$ value was of 82.6 $mM^{-1}s^{-1}$ for $T_2$-weighted MRI. As $T_1$ and $T_2$ are known to rely on the number of Gd(III) ions or the size,[100] the dense multi Gd(III) complex, represented as nanogel, resulted in a transverse relaxivity that lay in the range of SPIONs. Finally, these nanogels should be considered as potential candidates for theranostic purposes since the bPEI core surface could be easily modified with suitable drugs and bioactives molecules.

A study that tested different chelators for efficient Gd nanogel formation was recently performed by Lux et al.[101] They designed polyacrylamide (PAAm) based nanogels with different acrylic DOTA (1,4,7,10-tetraazacyclododecane-1,4,7,10-tetraacetic acid) and DTPA based Gd(III) chelate complexes as crosslinker. Similar to the work of Soleimani et al.,[91] $r_1$ relaxivities in the range of 9.7 – 17.6 $mM^{-1}s^{-1}$ were obtained which were 3-4 fold higher than values of commercially available agents such as Magnevist® (Table 2). Since Gd(III) ions were embedded by crosslinking in the nanogel matrix, DTPA-based nanogels were more inert against transmetallation than Magnevist®, suggesting that crosslinker chelates may represent an important approach towards stable metal-chelating biomedical agents. As this methodology appeared in two steps, namely, the acrylic chelate Gd(III) complex formation followed by free radical emulsion polymerization with PAAm, an incorporation of the crosslinkers into nanogels with a biocompatible and biodegradable polymer backbone might be a promising perspective towards clinical relevance.

As shown in this section, most of the presented nanogel based MRI contrast agents are still in the preliminary stage of *in vitro* and *in vivo* testing. Several key issues have to be addressed to provide nanogel based MRI contrast agents with clinical relevance. These

issues mainly deal with pharmacokinetics, long-term stability, and toxicological effects. Therefore, intensive research is necessary to accomplish the ultimate task of using nanogel based MRI contrast agents for molecular and bio-imaging and thus achieve the transition of these concepts from bench to the bedside.

### 2.3. Other nanomaterials-nanogels: quantum dots, porous silica nanoparticles, and nanostructured carbon materials

As shown in Subsections 2.1 and 2.2, plasmonic and magnetic nanoparticles have been playing a significant role in the development of novel stimuli-responsive nanogel composites for potential application in nanomedicine. In addition to these examples, a great deal of effort has been devoted to creating new types of nanomaterial-nanogel composites with enhanced functions, including the use of QDs, porous silica nanoparticles (PSNPs), and nanostructured carbon materials (Table 3). This section highlights the features of such nanomaterials as part of stimuli-responsive hybrid nanogel systems and their applications for delivery of therapeutic agents.

**Table 3.** Summary of the most recent and significant studies on incorporating nanomaterials into nanogel composites for their use in nanomedicine.

| Nanomaterial: QDs, PSNPs, and nanostructured carbon materials | Polymer network | Preparation methods | Stimuli | Enhanced property and application | Ref. |
|---|---|---|---|---|---|
| Protein coated-QDs | CHPN$H_2$ | Self-assembly of negatively charged QDs and positively charged | - | - | 113 |

| | | | | | |
|---|---|---|---|---|---|
| | | nanogels | | | |
| MPA-capped CdTe QDs | Chitin | Incorporation of QDs into preformed nanogels | pH | pH-sensitive drug delivery system with simultaneous biosensing | 114 |
| MPA-capped CdTe QDs | PNIPAm | Copolymerization of MPA-QDs during PNIPAm polymerization | Temperature | Temperature dependent on–off fluorescence properties | 115 |
| CdS QDs | p(NIPAm-AAm-PBA) | *In situ* immobilization of QDs within the microgels | Temperature and [glucose] | Non-invasive continuous optical detection of saccharides | 116 |
| CdSe-ZnS core-shell QDs | Polypeptide | Self-assembly of QDs and polypeptide complex | pH and temperature | Targeted nanogel for simultaneous cancer diagnosis, imaging, and therapy | 41 |
| $Bi_2O_3$ QDs | PVA | *In situ* immobilization of QDs within nanogel-network | Temperature | Temperature-responsive anticancer drug release with dual-model imaging for theranostic actions | 122 |
| Hollow silica | PNIPA | Crosslinking | Temperat | Enhanced stability | 134 |

| | | | | | |
|---|---|---|---|---|---|
| spheres | m | polymerization | ure | and well-controlled drug release | |
| Silica nanoparticles | Poly(N-isopropylacrylamide-co-2-(dimethylamino) ethyl methacrylate, methyl-chloride) | Surfactant-free emulsion polymerization | Temperature | Controlled slow drug release of more than 24 h | 133 |
| PSNPs | P(VCL-s-s-MAA)) | Precipitation polymerization in presence of the functionalized PSNPs | pH and temperature | Controlled pH- and temperature-triggered DOX release | 135 |
| PSNPs | PNIPAm | *In situ* radical polymerization in mesopores | Temperature | Temperature-responsive controlled ibuprofen delivery | 136 |
| PSNPs | alginate/CHI | layer-by-layer self-assembly | pH | pH-responsive DOX release | 137 |
| Fullerene ($C_{60}$) | DMA-GC | Self-assembly of chitosan-based polymer | Light | Advanced endosomal pH targeting for photodynamic | 26 |

| | | | | | |
|---|---|---|---|---|---|
| | | and $C_{60}$ | | antitumor therapy | |
| f-SWCNTs | PVI-*co*-AA | Crosslinking polymerization | pH | Improved thermal stability of the pH-sensitive nanogel composite | 23 |
| CHI-CNT | PNIPAm | Crosslinking polymerization | NIR light and temperature | Triggered DOX release upon NIR irradiation | 155 |
| rGO | PNIPAm/ PEG-d/ chitosan | Crosslinking polymerization | NIR light and temperature | Improved photothermal response resulting in a fast drug release | 163 |
| PEI-coated NDs | N-acetylated chitosan | Crosslinking polymerization | Enzime-responsive | Enhanced mechanical properties | 168 |

### 2.3.1. Quantum dots@nanogels

To fulfill the need for tracking certain biomolecules or cells by *in vitro*/*in vivo* imaging, development of specific biocompatible labels is an inevitable task for the study and understanding of the role of novel drug delivery systems. In this regard, QDs-containing nanogel composites have been reckoned as desirable inorganic-organic hybrid material in optical sensing and imaging due to their intriguing luminescence characteristics and electronic properties of QDs such as bright fluorescence, broad absorption with narrow symmetric emission spectra, remarkable photostability, and biocompatibility.[102-110] QDs are nanometer-order semiconductor crystals that exhibit discrete energy levels and their

electronic and optical properties are determined only by their size. Depending on their diameter, QDs therefore shine in different colors when exposed to ultraviolet light, (e.g., blue = 2 nm QDs; red = 6 nm QDs).[111, 112]

In the last few years, different strategies have been used to obtain stimuli-sensitive QDs-based fluorescent probe nanogel composites as drug delivery systems with simultaneous imaging and biosensing. A simple approach is to incorporate surface-modified QDs into the polymer network of the preformed nanogels. For example, Hasegawa et al. prepared monodisperse hybrid nanoparticles of 38 nm by mixing protein-coated QDs with amino-modified cholesterol-bearing pullulan nanogels ($CHPNH_2$–QD) in phosphate buffered saline (PBS) solution for 30 min at room temperature.[113] Although the incorporation of QDs into unmodified, neutral cholesterol-bearing pullulan (CHP) nanogels was suppressed, electrostatic interaction between negative charged QDs and positively charged amino-containing nanogels induced the successful formation of the hybrid nanogel complex. Furthermore, the QDs@$CHPNH_2$ nanogel composite did not form aggregations after their internalization into various human cells. In a similar way, Rejinold et al. reported the preparation of multifunctionalized biodegradable nanogels by simply mixing mercaptopropionic acid-capped CdTe QDs and chitin nanogels in an aqueous solution.[114] The unreacted -OH and -$NH_2$ groups of the repeating N-acetylglucosamine units, that compose the chitin chains, acted as anchor points to sequester $Cd^{2+}$ ions and further immobilize CdTe QDs into the nanogel matrix. The obtained CdTe QDs-chitin nanogel composite as fluorescent probe and drug delivery system could be easily loaded with bovine serum albumin (BSA) showing promising applications for simultaneous bioimaging during drug release under local environmental conditions. Under the same trend, different nanogel networks have been used to seize QDs in nanomedicine as sensing and imaging materials.[115-117] Nevertheless, the design of multitasking hybrid drug carriers capable of

integrating various functionalities in one single nano-object is highly desirable.[118-120] Recently, Yang et al. developed an interesting QDs@polypeptide nanogel composite with a dual hydrophilic/hydrophobic character (Figure 5).[41] The main formation of the novel hybrid nanogels can be summarized in two steps: (a) specific metal-affinity interaction between hydrophilic glutathione-coated CdSe-ZnS QDs with N-terminal polyhistidine sequences of PC10A or PC10ARGD coiled-coil polypeptides and (b) nanogel formation and final encapsulation of QDs via self-assembly. The thus obtained pH and temperature dual responsive QDs-polypeptide nanogels of 23 nm in diameter were further loaded simultaneously with hydrophobic and hydrophilic dyes (2-amino-4,6-bis-[(4-N,N'-diphenylamino)styryl] pyrimidine and fluorescein sodium, respectively) as model drugs. Their evaluation in HeLa cancer cells revealed remarkable overexpressed $\alpha_v\beta_3$-integrin receptors for simultaneous optical pH-sensing and targeted delivery of drugs.

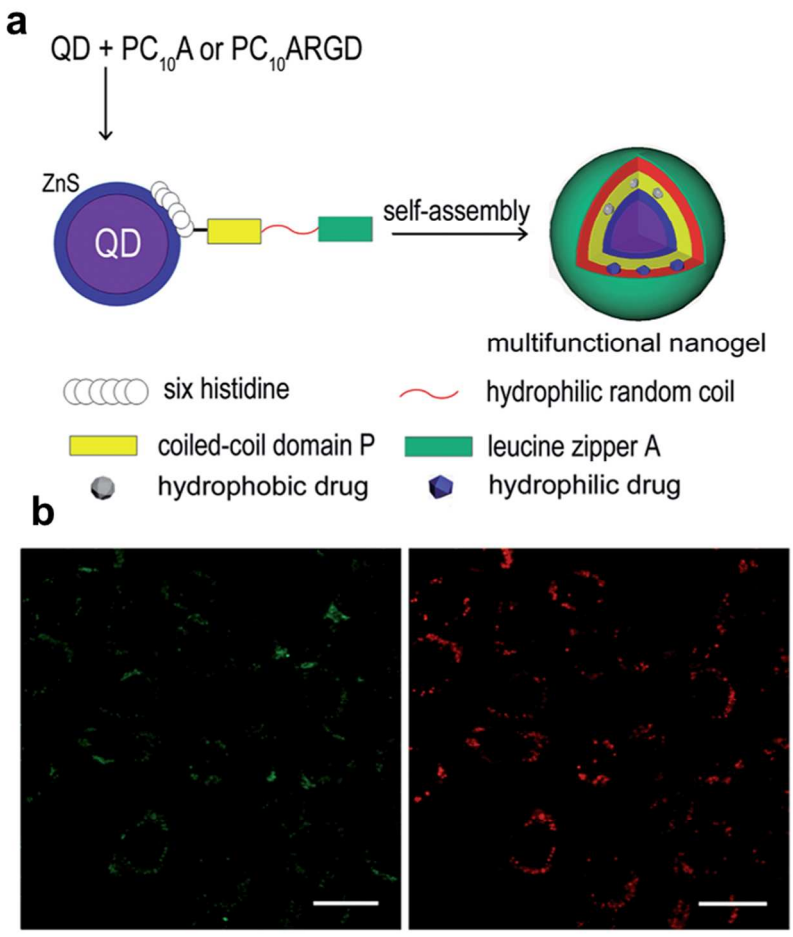


**Figure 5.** (a) Schematic representation of QDs@polypeptide nanogel. (b) Confocal fluorescence images of HeLa cells incubated with QDs@polypeptide nanogel, green and red channels showed the green dye (fluorescein sodium) signal and red QDs signal. Reproduced from Ref. 41 with permission from The Royal Society of Chemistry.

Other strategy for the preparation of QDs@nanogel composites can be the *in situ* synthesis of QDs in the interior of the nanogel. This approach has been illustrated by Wu et al.[121] by conducting a successful *in situ* synthesis of CdSe QDs inside of a temperature- and pH-sensitive polysaccharide-based nanogel network. In the construction of a hybrid QDs-nanogel complex, the synthesis of QDs within gel-matrix offered a confined growth process that could improve chemical interaction of quantum nanocrystals with the polymeric gel to confer them optimal dimensions and stable optical signal. Following a

similar strategy, Zhou's group moved forward in their research and developed pH sensitive CdSe@CHI-poly(methacrylic acid) and temperature responsive $Bi_2O_3$@PVA nanogels by *in situ* formation and immobilization of QDs.[122, 123] The main goal of such custom-designed engineering nanohybrid systems was to integrate multifunctionalties for simultaneously biosensing, bioimaging, and effective therapy.

### 2.3.2. Porous silica nanoparticles@nanogels

PSNPs have received significant attention in the last decade because of their superior and tunable physicochemical properties making them ideal in many fields of application such as catalysis, adsorption, sensors, and biomedical technology.[124, 125] PSNPs are particularly attractive as drug delivery systems owing to their large surface area, tunable pore size, non-toxic nature, facile surface functionalization, high loading and controlled drug release, and excellent biocompatibility.[126-132] Although the stimuli-responsive silica-based nanogels can be a fascinating subject of study, few works in this topic have become known in the recent years. Chai et al. reported a surfactant-free emulsion polymerization and biomimetic template approach for the synthesis of thermoresponsive hybrid nanogel-silica core–shell particles.[133] Poly(N-isopropylacrylamide-co-2-(dimethylamino) ethyl methacrylate, methyl-chloride) quaternized nanogel particles were *in situ* covered with silica and the obtained nanogel-silica particles were further loaded with aspirin. The drug delivery nanogel-silica system showed a controlled slow drug release of more than 24 h, while the non-templated silica nanogel practically released its cargo within 5 h. This work demonstrated that nanogel particles covered with a silica shell can effectively retard or control the drugs release.

Motivated by the potential application of spherical hollow silica matrices, Liu et al. constructed a thermoresponsive drug release system based on hollow silica nanospheres coated with a PNIPAm nanogel shell.[134] The prepared hollow silica nanogels showed good

biocompatibility under *in vitro* cytotoxicity evaluation as well as excellent thermoresponsive controlled-release behavior of Rhodamine B (RHB) during release studies. This hollow silica PNIPAm-nanogels can be highly suitable for stimuli-responsive controlled-release drug delivery applications. Similar systems have been performed using nanostructured mesoporous silica covered with stimuli-responsive polymer shells in order to retard and control the release rate of the cargo under environmental stimulus control.[135-137] The development of hollow or mesoporous silica materials offers new possibilities for incorporating specific drugs within silica cavities followed by controlled release of its cargo from the matrix due to its well-defined structure.

### 2.3.3. Nanostructured carbon materials@nanogels

Over the past several decades, nanostructured carbon materials in various allotropic forms (e.g., fullerenes, nanotubes, graphene, and diamonds) have received overwhelming attention because of their unique physical and chemical properties tunable in a wide range, such as high specific surface area, narrow pore width, large pore volume, low density, excellent electronic conductivity, and high thermal and mechanical stability.[138-140] Considering such features, carbon-based nanostructured materials have been extensively studied in many different fields, including energy conversion and storage, catalysis support, adsorption, gas storage, water treatment, and more recently biomedicine.[141-143] The use of nanostructured carbon materials with tunable functionalities promises great advances in drug delivery and therapeutic treatment.[22, 144-146] For example, the spherical fullerene $C_{60}$, also known as buckminsterfullerene,[147] has been considered as a photosensitizing agent for non-invasive photodynamic therapy treatments owing to its photo-physical abilities to absorb energy at a specific wavelength in the UV range and to further transfer the excited energy to oxygen molecules, resulting in the generation of

cytotoxic agents (singlet oxygen).[148-150] Recently, Kim et al. synthesized a photo-responsive $C_{60}$@glycolchitosan-based nanogel composite via self-assembly of 2,3-dimethylmaleic acid-grafted glycol chitosan chains and $C_{60}$ nanoparticles.[26] This hybrid nanogel showed an innovative ability for endosomal pH targeting, through an enhanced singlet oxygen generation and high photodynamic tumor cell ablation at pH 5.0. This system displayed great capability for its use in selective endosomal delivery of photosensitizer drugs for tumor cells.

Despite the interesting properties of the fullerenes, the spotlight of scientific research has focused on the utilization of other nanostructured carbon materials in recent years. In terms of mechanical, optical, conductive, and thermal properties, carbon nanotubes (CNTs) have received enormous attention in the field of bioapplications.[151-153] Although many research groups have incorporated CNTs into hydrogel polymers[154] in order to reinforce gel structure, increase electrical conductivity, and enhance NIR sensitivity properties, only few works have reported the preparation of CNTs-nanogel composite for drug delivery purposes.[23, 24, 155] Nevertheless, this is a topic that will be much studied in forthcoming years. Very recently, Qin et al.[155] published the development of a NIR triggered DOX delivery system based on CHI-coated CNT encapsulated in a PNIPAm nanogel (PNIPAm@CHI-CNT, Figure 6). In this work, they reported a high DOX loading capacity of ~ 43% and a faster drug release at 40 °C and pH 5. Moreover, due to the CNT these nanogels showed a triggered DOX release upon NIR irradiation.

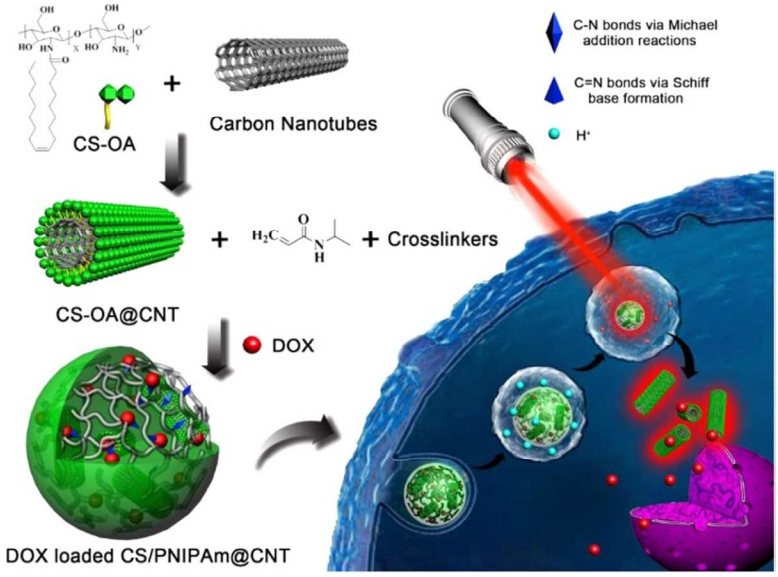


**Figure 6.** Schematic representation of DOX loaded PNIPAm@CHI-CNT and the triggered drug release by NIR irradiation. Reprinted from Ref. 155, Copyright (2015), with permission from Elsevier.

Although CNTs have been actively researched for their possible application in nanomedicine since the late 90s, graphene has garnered tremendous attention in biomedicine in the past few years because of its high mechanical strength, great optical absorbance, excellent thermal conductivity, and low toxicity.[156-159] Graphene is a sheet-like two-dimensional $sp^2$-bonded carbon structure and a single layer of graphene sheet has a thickness of 0.34 nm (one-atom thick). Particularly, reduced graphene oxide (rGO) is capable to adsorb NIR light and convert such optical energy into thermal energy.[160-162] Under this consideration, Wang et al. constructed a photothermal NIR light-responsive drug delivery platform based on CHI-modified rGO crosslinked with NIPAm and polyethylene glycol-diacrylate (PEG-d).[163] The rGO hybrid nanogel was further loaded with DOX as an anticancer drug showing high loading capacity up to 48 wt%. *In vivo* studies showed that the photothermal response of the rGO to NIR irradiation led to a rapid rise in the temperature of the surrounding gel and resulted in a fast release of the loaded DOX

with high local controllability. The weight composition of rGO/nanogel not only had a dramatic effect on the thermo- and photo-responsive properties of the hybrid nanogel composite, but also a defect or excess in rGO could switch-off or switch-on a specific skill of the rGO-nanogel complex.[161] For example, at a rGO composition of ~47.5 wt%, the nanogel composite showed both thermo- and photo-sensitivities, while at lower (≤32 wt%) or higher (≥64.5 wt%) rGO composition the hybrid nanogel only presented thermal- or photo-sensitive properties, respectively. Furthermore, an excess of rGO (≥78.5 wt%) caused the nanogel composite to lose its responsive properties.

Lately, a particular allotropic form of carbon has been considered for its use in bioimaging, biosensing, and therapeutic applications: diamond. Particularly, nanodiamonds (NDs) are three-dimensional $sp^3$-bonded carbons with distinctive faceted surface architecture where, depending on the size and morphology, the $sp^3$-surface of the NDs is stabilized through either termination with functional groups or reconstruction of $sp^3$ carbon into $sp^2$ carbon. The presence of such surface functional groups on the NDs allows i) to coordinate water molecules around the surface and ensure well-dispersion in an aqueous media/matrix and ii) to interact chemically with specific molecules or drugs in a biocompatible environment.[164, 165] Furthermore, NDs have been demonstrated excellent biocompatibility under many *in vitro* and *in vivo* studies.[166, 167] Very recently, the rational design of therapeutic contact lenses through the incorporation of NDs into nanogel matrices as effective ocular drug delivery platforms has been demonstrated by Kim et al.[168] They have synthesized a drug-loaded ND@nanogel composite via crosslinking polyethyleneimine-coated NDs and partially N-acetylated CHI in the presence of timolol maleate. The timolol-containing NDs@nanogels were then embedded within a hydrogel matrix and cast into enzyme-responsive contact lenses (Figure 7). The main role of the coated NDs is to retain the timolol by short distance chemical interactions and to avoid the prematurely elution of

the drug, but keeping it physically active for its further release under degradation of the nanogel via lysozyme cleavage. In addition to the improved timolol-controlled release, the incorporation of a small amount of NDs into the lens matrix enhances tensile strength and boosts elastic modulus by the reinforcement of the polymer matrix. Overall, the obtained lysozyme degradable, timolol-loaded ND@nanogel embedded contact lenses not only had excellent water and oxygen permeability, optical clarity, and improved mechanical properties, but most importantly also displayed sustainable drug release under lysozyme activation. This novel NDs-based system provided an interesting platform for the development of advanced enzyme-triggered drug release devices for sustained therapy applications.

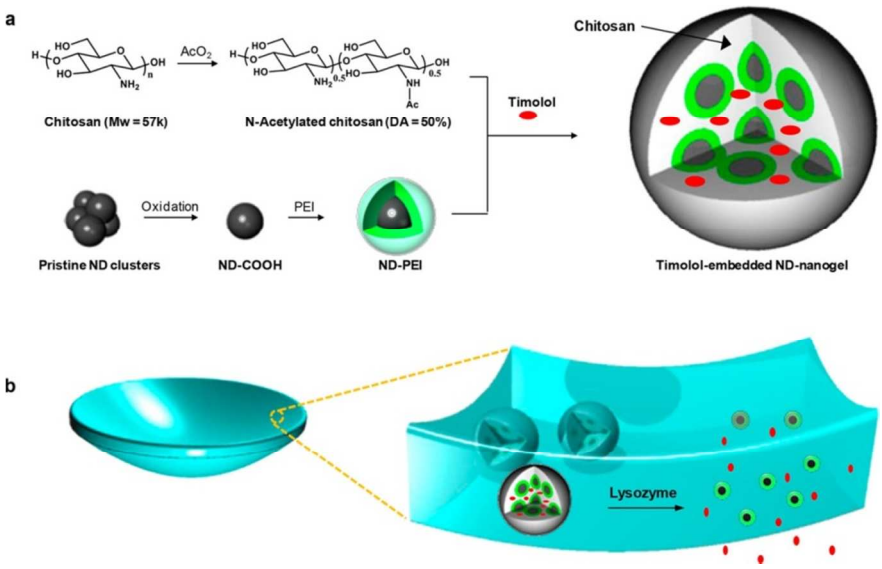


**Figure 7.** Schematic representation of (a) timolol-loaded ND@nanogel and (b) ND@nanogel embedded contact lenses. Reprinted with permission from Ref. 168.

Undoubtedly, the use of QDs, PSNPs, and nanostructured carbon materials to control mechanical, optical, electrical, and thermal properties of smart nanogel composites for potential on-demand high-controlled drug delivery nanovehicles have made tremendous advances in nanomedicine. However, the capability of the nanomaterials, mentioned in

this section, to enhance hybrid nanogel composite abilities is still not fully explored. We believe that forthcoming research on the topic and further full-understanding of biological systems will change dramatically today's concepts and a huge progress in biomedical technology will take place in a near future.

## 3. Polymer-nanogels composites

Composites of nanogels with other polymers not only extend the applicability of these systems due to the multisensitiveness,[169] but moreover overcome some disadvantages of single networks as, for example, slow-rate response,[170] the hysteresis during repeated swelling–shrinking cycles,[171] etc. Based on the nature of the composite polymer-nanogels can be classified in two categories (a) IPNs networks and (b) core-shell particles. The utilization of these strategies for obtaining multiresponsive hybrid nanogels and their further application in nanomedicine will be described in the following sections (3.1 and 3.2).

### 3.1. Interpenetrated and semi-interpenetrated polymer networks

To enhance the mechanical strength, the swelling/deswelling response, and to add new sensitivities to a nanogel, multicomponent networks as IPNs have been designed (Table 4). IPNs are defined by IUPAC as “two or more networks that are at least partially interlaced on a molecular scale but not covalently bonded to each other and cannot be separated unless chemical bonds are broken”.[172] The combination of the polymers results in a polymeric system with a new profile. IPN networks can be classified in fully-IPN (IPN)[173] when the interpenetrated polymer is crosslinked inside the first network, or in semi-IPN (sIPN)[27] when a linear polymer is embedded within the first network.

There are two synthetic pathways for obtaining IPN networks[174] (1) simultaneous IPN, where both monomers are mixed and the polymers synthesized at the same time by noninterfering routs [175] and (2) sequential IPN, where the second monomer is polymerized *in situ*, inside the first single network.[176]

**Table 4.** Interpenetrating polymer networks in nanomedicine.

| Network | Polymers | Stimuli | Application | Ref. |
|---|---|---|---|---|
| IPN | PNIPAm/PAA | Temperature and pH | Stomach-specific drug delivery system | 31,173,178 |
| sIPN | HPC/PAA | Temperature and pH | Oxaliplatin delivery | 180 |
| IPN | CHI/POEG | Temperature and pH | Chemo-cryo cancer therapy | 182 |
| IPN | P(NIPAm–Dex–PBA) | Temperature and [glucose] | Insulin delivery | 170,220 |
| IPN | [P(NIPAm-co-FPBA)]/PAAm | Temperature and [glucose] | Nanoglucometer | 171 |
| IPN | NaAlg/PAA | pH | Ib controlled release | 184 |
| sIPN | CHI/PMAA | pH | TMZ release | 123 |
| IPN | PNIPAM/PAA | Temperature and pH | Imaging by SERS | 185 |

One of the major uses of IPN networks is obtaining biomedical relevant dual responsive hybrid nanogels with little interference between stimuli.[31] Several examples of IPNs for synthesizing dual pH/temperature responsive networks as drug delivery systems were published in the last decade.[27, 173, 177-180] do Nascimento Marques et al.[181] found that the introduction of pH-sensitive polymers to crosslinked PNIPAm particles not only produced dual-sensitive materials but also allowed particle stability to be adjusted depending on the

desired application. In this context, Xing et al.[173] reported temperature/pH dual stimuli responsive hollow nanogels with an IPN structure based on a PAA and PNIPAm (PNIPAm/PAA IPN hollow nanogels). These nanogels showed a high drug loading capacity of Isoniazid (INH), an antitubercular drug, up to 668 mg INH per gram of the nanogel. *In vitro* drug release studies showed an acid triggered drug release behavior, thus making them a potential stomach-specific drug delivery system.

Besides PNIPAm, other thermoresponsive polymers were used in IPNs networks. Chen et al.[180] reported the synthesis of thermo and pH dual-responsive nanogel of hydroxypropylcellulose-poly(acrylic acid) (HPC-PAA) particles with sIPN polymer network structure. The novelty of this system was that depending on the chemical composition and the degree of crosslinking, the thermoresponsive behavior could be shifted from the upper critical solution temperature (UCST) to the LCST. Additionally, oxaliplatin was successfully loaded in the nanogel showing a high *in vitro* anticancer activity.

Another thermoresponsive system, based on poly(oligo ethylene glycol) (POEG), was used by Zhou et al.[182] who combined the advantages of linear PEG and temperature-responsive polymers in a single macromolecular structure. They have designed a new class of pH-responsive CHI-based nanogels by IPN of CHI chains into a POEG chain network (Figure 8). The POEG-CHI nanogels responded to the changes in environmental pH and the cell internalization is facilitated by the positive surface charge of the nanogels in the tumor extracellular pH (~6.0–6.2). More interesting, the IPN enabled a remote modulation of the pH response by external cooling/heating (cryo/thermo treatment). The nanogel was loaded with 5-FU, a model anticancer drug, which could be released from the drug carriers upon the increased acidity in subcellular compartments (~5.0). The *in vitro* studies in B16F10 melanoma cells showed reduced toxicity in combined chemo-thermo

treatments but significantly enhanced therapeutic efficacy in combined chemo-cryo treatments.

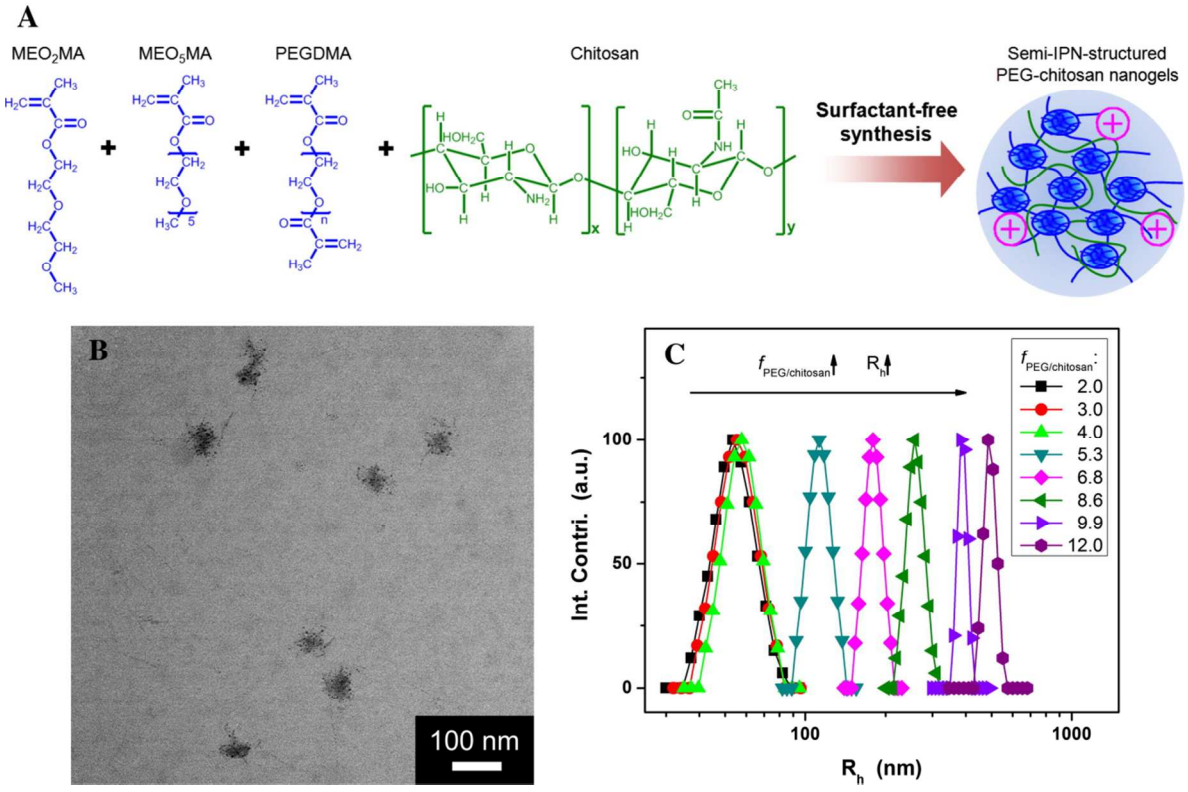


**Figure 8.** (A) Schematic illustration of POEG-chitosan nanogels with a semi-IPN structure. (B) TEM images of POEG-chitosan nanogels. (C) Effect of mol ratio fPOEG/CHI values on the average hydrodynamic radius (Rh) of POEG-CHI nanogel particles. Reprinted from Ref. 182 with permission from John Wiley & Sons, Inc..

Additionally, the IPN strategy was extensively studied for the production of glucose sensitive nanogels in order to address the slow-time-response issue of the other insulin delivery systems reported previously.[183] Wu et al.[170] reported the synthesis of a nanogel dispersion with three interpenetrating polymer networks consisting of PNIPAm, Dex, and poly(3-acrylamidophenylboronic acid) (P(NIPAm–Dex–APBA)). The particle size could be

tuned with the Dex content. Their swelling behavior at different glucose concentrations revealed their sensitivity to glucose. Furthermore, the nanogels had good biocompatibility with L-929 mouse fibroblast cells. The loading amount of insulin was 16.2%, whereas drug release was dependent on the composition of Dex and the glucose concentration in release medium. *In vivo* experiments have shown the efficacy of the insulin-nanogels to decrease the glucose levels in blood of diabetic rats and the hypoglycemic effect of the insulin-nanogels was similar to the free insulin. They have further studied diabetes and developed a nanoglucometer based on a fluorescent hybrid nanogel glucometer (FNG) for intracellular glucometry.[171] This nanogel contained ZnO QDs covalently bonded onto a crosslinked network of PAAm, which was interpenetrated in a network of poly(N-isopropylacrylamide-co-2-acrylamidomethyl-5- fluorophenylboronic acid) [poly(NIPAm-co-FPBA)]. This double-network-structured FNG responded to the glucose levels of the surrounding media and converted the disruptions in homeostasis of glucose level into fluorescence signals at a fast time response. The high sensitivity and selectivity together with the good penetration in model B16F10 cells showed the promise of the FNG for the application as a nanoglucometer. In this example, the IPN strategy was used in order to overcome the problems during repeated swelling–shrinking cycles that are inherent to the simple networks systems.

Another application of the IPN strategy was the modification of the release profile of different drugs.[123, 184] In this context, Babu et al.[184] developed a pH-sensitive IPN network of sodium alginate (NaAlg) and AA for controlled release of Ibuprofen (IB). While NaAlg disintegrated in the intestinal fluid, PAA provided pH-sensitivity to the nanogel.

Wu et al.[123] reported the synthesis of hybrid nanogels based on the inmobilization of CdSe QDs in poly(methacrylic acid) (PMAA) networks sIPN with CHI. They have shown that the crosslinked structure conferred colloidal and structural stability compared with the non

crosslinked hybrid nanogels. The covalently crosslinked hybrid nanogels proved to have neglectable cytotoxicity, could sense the environmental pH change, and regulated the release of anticancer drug, temozolomide (TMZ), in the typical abnormal pH range of 5-7.4.

Very recently, a new application of the IPN strategy was developed by Liu et al.[185] They have synthesized an AgNP-loaded PNIPAM-PAA interpenetrated microgel for its use in surface-enhanced raman scattering (SERS). SERS is an optical detection technique whit higher sensitivity than traditional techniques and, more importantly, it can be used for detection in blood and other biological environments.[186] In this work, they have proved that the SERS intensity can be reversibly tuned with temperature or pH, showing an increment when lowering the pH from 7 to 3 or rising the temperature from 20 to 45 °C. With this study, new opportunities in the field of theranostics are open.

### 3.2. Core-shell polymer networks

Nanogels with core-shell architectures were designed to yield separate but covalently bound compartments, which result in inhomogeneous but chemically stable single particles. This inhomogeneity can be exploited for the design of nanogels that respond to multiple signals. Typical examples describe thermoresponsive nanogels exhibiting more than one phase transition temperature,[169, 187] amphoteric nanogels that swell in both basic and acidic media but shrink near the isoelectronic point,[188] nanogels that are both thermo- and pH-responsive,[133, 169, 188-192] core-shell nanogels with controlled drug delivery,[193, 194] etc.

The grafting of specific (macro-)molecules to the core of nanogels was used to yield star-like core-shell nanogels, which are active towards enhanced cell epitope recognition[30, 195, 196] or increased protein resistance of the nanogels.[197-201] PEGylated nanogels are the most common example of core-shell nanogels in which PEG acts as the shell. The grafting of

linear PEG chains on the surface of the nanogels contributes to a drastic increase in the bioavailability of the particle due to the protein-resistant properties of PEG.[202] Its use is widespread due to its approval by the Food and Drug Administration (FDA) for pharmacological use. The readers are referred to the review by Knop et al. for a more comprehensive discussion of PEG as shell for drug delivery applications.[202]

A review by Richtering and Pich extensively discussed the peculiar swelling properties of stimuli-responsive core-shell nanogels.[203] It was observed that the mechanical properties of such particles are determined by both core and shell, which are dynamically influencing each other. The architecture of core-shell particles is conferring physical constrictions to the swelling of the two single compartments. This leads to varied LCSTs as well as swelling degrees.

In the pioneering work of Jones and Lyon,[189] which reported in 2000 the first example of a core-shell nanogel, it is observed that the shell swelling behavior plays a major role on the swelling of the whole particle. This effect is especially observed when a charged PNIPAm-co-AA polymer is in the shell rather than its uncharged PNIPAM counterpart. When added the shell, the decreased interchain distance in the core polymer leads to decreased LCST as well as lower swelling degree.

Since then, a wide number of studies have been published in this field describing the synthesis and characterization of core-shell nanogels. A review by Hendrickson et al.[204] in 2010 already described multifunctional core-shell nanoparticles. We will therefore preferentially focus our attention on more recent papers regarding core-shell nanogels applied in nanomedicine. A number of studies reported the synthesis and characterization of novel core-shell nanogels, as they are listed in Table 5.

**Table 5.** Summary of the most recent and significant studies on core-shell nanogels

| Core | Shell | Responsiveness | Ref. |
|---|---|---|---|
| P(NIPAm-co-CMA) | P(DMA-co-CMA) | Temperature (LCST NIPAm + UCST nanogel) | 187 |
| P($MeO_2$MA) | P($MeO_2$MA-co-OEGMA) | Temperature (2 LCST) and pH | 169 |
| P(IADME-co-VIm) | P(VCL) | Temperature, pH (amphoteric) | 188 |
| OEG | OEG or PEG | Temperature | 200 |
| PEAMA | PEG | pH | 201 |
| Poly(DVB)-co-(PEG, NIPAm, MBA, MPA) | PNIPAm-co-(MBA, MPA) | Temperature | 207 |
| OEG | PEG | Temperature | 208 |
| BAP | PEG | Reducing conditions | 210 |
| PEAMA | PEG | pH | 211 |

The synthesis of core-shell nanogels was reported following different procedures. The most common technique is the seed precipitation polymerization, in which the already prepared thermoresponsive core is used in its collapsed state for the growing of the shell on its surface via a second step of radical polymerization.[30, 188, 189, 191, 195, 196, 205] Another widespread synthetic technique is the crosslinking of amphiphilic micelles preformed by self-assembly[133, 187, 192, 197, 206] or the reversible addition−fragmentation chain-transfer polymerization (RAFT).[169, 187, 190, 200, 206-208] All these synthetic methodologies can give core-shell nanogels with facile scalability and low polydispersity.

The imaging of core-shell nanogels was typically performed via transmission and scanning electron microscopy (TEM, SEM)[133, 169, 187-189, 191, 198, 199, 206, 209, 210] or atomic force microscopy (AFM).[192, 200, 208, 209] The visualization of the two distinct compartments in

polymer-only core-shell nanoparticles is usually problematic due to the soft properties of these materials. Nevertheless, TEM and AFM microscopy provided some nice micrographs of core-shell nanogels displaying the distinct environments, as shown in Figure 9.[189, 191, 192] The data obtained by the characterization via small-angle X-Ray scattering (SAXS) and small-angle neutron scattering (SANS) was used to determine radial structural information for the nanogels. The data was fitted to a concentric core-shell model function to give a more accurate description of the size of core and shell compartments.[197, 201, 211]

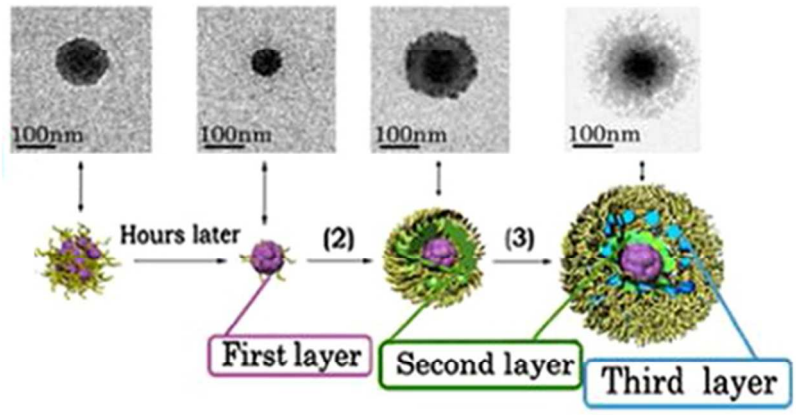


**Figure 9.** TEM image of the controlled formation of microgels/nanogels. Adapted with permission from Ref. 210. Copyright (2012) American Chemical Society.

Among other biomedical applications, several studies were conducted for the synthesis of core-shell nanogels as effective carriers for short interfering ribonucleic acid (siRNA) delivery. An interesting review about this subject was published in 2012 by Smith and Lyon.[212]

Glucose-responsive core-shell nanogels were developed for the treatment of *diabetes mellitus*. Lapeyre et al.[205] and Zhao et al.[198] developed systems that efficiently prolonged

release of insulin in presence of elevated blood glucose levels. PNIPAm-based core-shell nanogels including a comonomerized glucose-responsive phenylboronic acid (PBA) derivative in the shell were synthesized.[205] It was found that PBA forms stable complexes with glucose, and as a result the increased hydrophilicity of the complex leads ultimately to the swelling of the nanogels. The synthesis of the thermoresponsive PNIPAm core occurred via precipitation polymerization, the collapsed cores were subsequently used as seeds for the second analogous polymerization step, which was performed to include the PBA derivatives APBA or 4-(1,6-dioxo)-2,5-diaza-7-oxamyl)phenylboronic acid (DDOPBA) as the glucose-responsive comonomer together with NIPAm. Core-shell nanogels obtained with DDOPBA were used for biological studies because of their higher biocompatibility at physiological pH, being the pKa of DDOPBA 7.8. The swelling behavior of the PNIPAm-APBA core-shell nanogels was extensively investigated in relation with glucose binding, and a complex behavior was observed. At temperatures below the LCST of PNIPAm (T = 32 °C), binding of glucose to the nanogels led to swelling of the shell, which then allowed the relaxation of the otherwise constrained core. Moreover, the swelling degree of the shell was found to be a tuned response, directly proportional to the glucose concentration. The results for PNIPAm-DDOPBA nanogels were found to be very similar to those of PNIPAm-APBA nanogels, although a higher transition temperature was observed in this case. The breathing-in technique was used to encapsulate FITC-insulin in the nanogels, and a prolonged retention of the drug was observed for the loaded nanogels. The release of insulin from PNIPAm-DDOPBA nanogels proved to be dependent on the presence of glucose over a 9 h time span, as shown from fluorescence spectroscopy.

Park et al.[197] reported the synthesis of pH-responsive, core-shell poly(aspartic acid)-PEG nanogels, which were also able to prolong the release of insulin. A linear block copolymer

of PEG-*co*-poly(succinimide) (PEG-*co*-PSI) was synthesized, which formed micelles via self-assembly. After micellation the PSI residues were crosslinked with hexamethylenediamine to form the precursor nanogel. Subsequently, an alkaline hydrolysis of the PSI core led to the formation of the poly(aspartic acid)-PEG nanogel (PAsp-PEG). Thus, the nanogel core turned hydrophilic and pH-responsive. The PAsp-PEG nanogels were incubated in a solution of recombinant human insulin, and its release from the nanogels was investigated. The release curve was found to be dependent on the pH, whereas the release was completed within 48 h at pH 7.4, while at pH 2 only 50% of the model drug was released in the same time span.

Analogous protein carriers were developed as core-shell nanogels. Chen et al. reported the synthesis of pH-responsive hollow core - porous shell PAA nanogels that exhibited surprisingly high loading capacities (800 wt% for BSA and 200 wt% for DOX).[209] The synthesis proceeded via the semi-interpenetration of PAA with HPC, the latter being removed in a subsequent step by alkaline hydrolysis, to give a core-shell nanogel of PAA alone. The removal of HPC left a void in the nanogel core. It was assumed that this structural organization was responsible for the very high loading capacities obtained after incubation of BSA and DOX. For BSA, the loading capacity was 8.0 mg per mg nanogel. Interestingly, TEM images showed that the BSA loaded nanogels became solid nanoparticles, while before encapsulation the nanogels had been soft materials. For DOX, the loading capacity (2 mg per mg nanogel) was lower than that of BSA, but nevertheless very high, if compared with the values obtained by other nanocarriers.[213] The release behavior for BSA was shown to be almost independent on the pH, indicating that the driving force of encapsulation and release was not of electrostatic nature, but dependant on hydrophobic interactions. Circular dichroism spectra proved that the native structure of BSA was retained after encapsulation and release. On the other hand, the release profile

of DOX was shown to be strongly dependent on the pH. At more acidic conditions (pH 4.0), the release of DOX was shown to be much faster than at a physiological pH of 7.4.

Another example of protein carrier was developed by Bhuchar et al.[206] Core-shell nanogels exhibiting a thermoresponsive poly(methoxydiethylene glycol methacrylate)-co-poly(2-amino-ethyl methacrylamide hydrochloride) (MeODEGM-co-AEMA) core and a shell of poly(2-methacryloyloxyethyl phosphorylcholine) were synthesized via a one-step RAFT. The resulting nanogels exhibited a thermoresponsive core with 2,2-dimethacroyloxy-1-ethoxypropane as the crosslinker, which degrades in acidic conditions. The nanogel loading occurred via incubation in a protein solution (BSA, insulin, or β-galactosidase). The cationic AEMA residues present in the core of the nanogels increased the binding affinity of the oppositely charged proteins. The release of proteins was investigated via BCA assay, and the observed rate increased with decreasing pH, as expected from pH-degradable nanogels. Moreover, the release rates were found to be dependent on the size of the proteins: the smaller the protein, the faster its release out of the nanogels. Table 6 recapitulates the most recent studies on core-shell nanogels with controlled drug release.

**Table 6.** Summary of the most recent and significant studies on core-shell nanogels with controlled drug release.

| Core | Shell | Responsiveness | Controlled release | Ref. |
|---|---|---|---|---|
| PNIPMAm | PNIPMAm-co-aminopropyl methacrylate-YSA peptide | Temperature | siRNA & chemosensitization to docetaxel | 30,192 |
| Poly(aspartic acid) | PEG | pH | Rh-insulin | 197 |
| PEG-co-poly(phenylboronic acid) | PEG | [glucose] | Insulin | 198 |
| Poly(l-cystine-co-γ- | PEG | Reducing | Indometacin | 199 |

| | | | | |
|---|---|---|---|---|
| benzyl-glutamate) | | conditions | | |
| PNIPAm | PNIPAm-co-4-(1,6-Dioxo-2,5-diaza-7-oxamyl) phenylboronic acid | [glucose], temperature | Insulin | 205 |
| Poly(methoxydiethylene glycol) methacrylate and poly(2-aminoethyl methacrylamide hydrochloride) | Poly (2-methacryloyloxyethyl phosphorylcholine) | Temperature responsive and pH degradable | BSA, insulin, β-galactosidase | 206 |
| PAA (hollow) | PAA (porous) | pH | Very high loading (800% BSA, 200% DOX) but slow release | 209 |

Wu et al. reported the synthesis of an enzyme-degradable polyphosphoester (PPE) core – galactosylated (Gal) PEG shell nanogel for the treatment of hepatic carcinoma (Figure 10).[214] The synthesis of the nanogels proceeded via ring-opening polymerization of 3,6-dioxaoctan-1,8-diyl bis(ethylene phosphate) (TEGDP) together with monomethoxy-PEG (mMePEG) chains, initiated by stannous octoate in dimethylsulfoxide (DMSO) at 60 °C. The resulting nanogels were coupled with lactobionic acid in presence of PEG-$NH_2$ residues, assisted by sulfo-NHS and 1-ethyl-3-(3-dimethylaminopropyl)carbodiimide (EDC) coupling agents, to give Gal-PEG chains. The galactosyl ligand on PEG was used to target the asialoglycoprotein receptor (ASGP-R), which is overexpressed in mammalian hepatocytes.[215] The nanogels were loaded with DOX and incubated with HepG2 cells at 4 °C to investigate the receptor binding of Gal-nanogels, and the flow cytometry data showed a remarkable increase of fluorescence for Gal-nanogels compared to the non-galactosylated ones. Addition of lactobionic acid to the cell enviroment showed a competitive inhibition of the binding of Gal-nanogels on the cell receptors. Induced hepatocarcinoma in rats was treated with DOX-loaded Gal-nanogels, and a decrease in

tumor mass was observed for DOX-loaded Gal-nanogels compared to all other samples and controls.

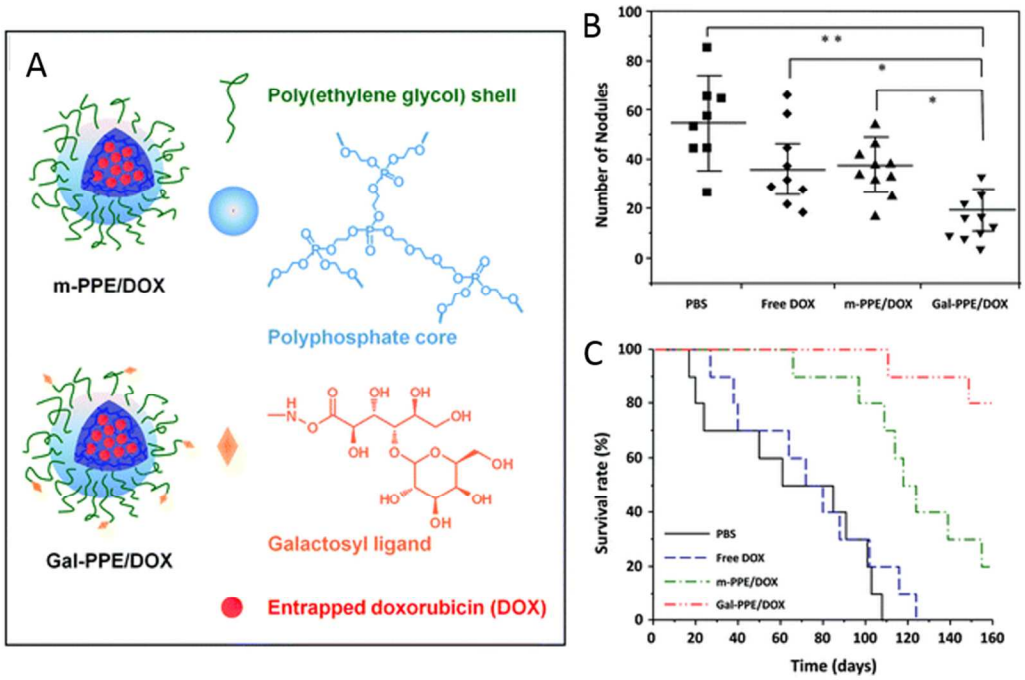


**Figure 10.** (A) Schematic representation of DOX-loaded Gal-nanogels. (B and C) *In vivo* studies on HCC-bearing rats after treatment with PBS, free DOX, m-PPE–DOX, or Gal-PPE–DOX. Adapted from Ref. 214 with permission of The Royal Society of Chemistry.

Moreover, biodegradable core-shell nanogels were reported by Xing et al. with the synthesis of a PEGylated poly(l-cystine-*co*-γ-benzyl-glutamate) nanogel via ring-opening polymerization.[199] The core was degradable under reducing conditions due to the presence of cystine residues. Interestingly, the reduction of the disulfide bonds of the cystine residues led to the formation of linear polymer chains rather than smaller products. This was due to the fact that the crosslinker was not present in the backbone of the nanogel but only on the single chains. The nanogels were loaded with the anti-inflammatory drug, indometacin, and a release study under both reducing ($10^{-2}$ M dithiothreitol (DTT)) and non-reducing conditions was conducted. The release of

indometacin was complete after 200 h under reducing conditions, while for non-reducing conditions a maximum release of 35% was observed after 80 h.

## 4. Preclinical and clinical development/application

Nanogel-based formulations have proven to be useful scaffolds in nanomedicine including drug delivery, anticancer therapy, imaging, etc., in *in vivo* animal models, but still many safety issues have to be overcome before the results can be applied to clinical practice. Without a doubt, cancer is one of the most challenging and studied application for hybrid nanogels, as was discussed in the previous sections and in numerous reviews.[216-219]

Nevertheless, hybrid nanogels were applied not only in anticancer therapies but in different medical applications like diabetes,[220] skin treatment,[221] cosmetics,[222] lenses,[168] vaccines,[223] neurosciences,[224] lupus,[25] etc. Table 7 summarizes the hybrid nanogels in preclinical and clinical trials.

Table 7. Hybrid nanogels in preclinical and clinical phase

| Phase | Hybrid nanogel | Application | Ref. |
|---|---|---|---|
| Preclinical | Plasmonic@NG | Cancer therapy | 69 |
| | Core-shell nanogels | Neurodegenerative disorders | 224-227 |
| | Core-shell nanogels | Treatment of acute pulmonary inflammation | 228 |
| | CHP-W9-peptide | Bone loss disorder | 237 |
| | CHP | Vaccines | 233,238,239 |
| Clinical | CHP | Vaccines | 234,235,240,241 |

Kavanov and Vinogradov[225] have extensively studied the use of nanogels for the treatment of neurodegenerative disorders in order to overcome the rapid clearance of the macromolecules injected in blood. They have developed cationic nanogels based on PEG and polyethylenimine for the systemic delivery of oligonucleotides (ODN) to the central nervous system.[226] Further studies proved that using the core-shell strategy for modifying the surface of those nanogels with polypeptides (transferrin or insulin) the permeability of the ODN increased two-fold.[227]

So far, the results of using the core-shell strategy in order to obtain a targeted therapy are promising for further clinical trials.[118] For example, Coll Ferrer et al.[228] designed a biocompatible nanogel composed of a Dex shell and a lysozyme core conjugated with an antibody (AntiICAM-1) directed to the pulmonary endothelium as a dexamethasone carrier to treat acute pulmonary inflammation in animal model of LPS-induced lung injury. *In vivo* studies demonstrated the therapeutic efficiency of ICAM-NG-DEX in mice while when a control nanogel was used; it did not have an anti-inflammatory effect of the encapsulated drug.

Despite great advances in the development and biological evaluation of nanogels, only few examples of clinical trials have been reported. The most advanced studies are for CHP nanogels. In 1991 Akiyoshi et al. showed that these hydrophobized polysaccharides form monodisperse and colloidally stable nanogels in water upon self-aggregation[229, 230] and that they have a strong binding for hydrophobic guest molecules,[231] proteins, and enzymes.[232] Since then, CHP nanogels have been used as drug delivery systems *in vivo* and in clinical trials, not only for cancer therapy[233-235] but also in treating Alzheimer's disorder,[236] for bone loss disorder,[237] and vaccines.[238, 239]

As an example of CHP preclinical studies, Nochi et al.[239] have used CHP nanogels as an intranasal vaccine-delivery system. In this work, they synthesized a non-ionic CHP

nanogel and a cationic, amino modified, CHP nanogel (cCHP) (Figure 11), thereby demonstrating that a neurotoxin BoHc/A administered intranasally with cCHP nanogel is effectively taken up by mucosal dendritic cells after its release (Figure 11b). Moreover, the hybrid nanogels did not accumulate in the olfactory bulbs or brain and induced tetanus-toxoid-specific systemic and mucosal immune responses.

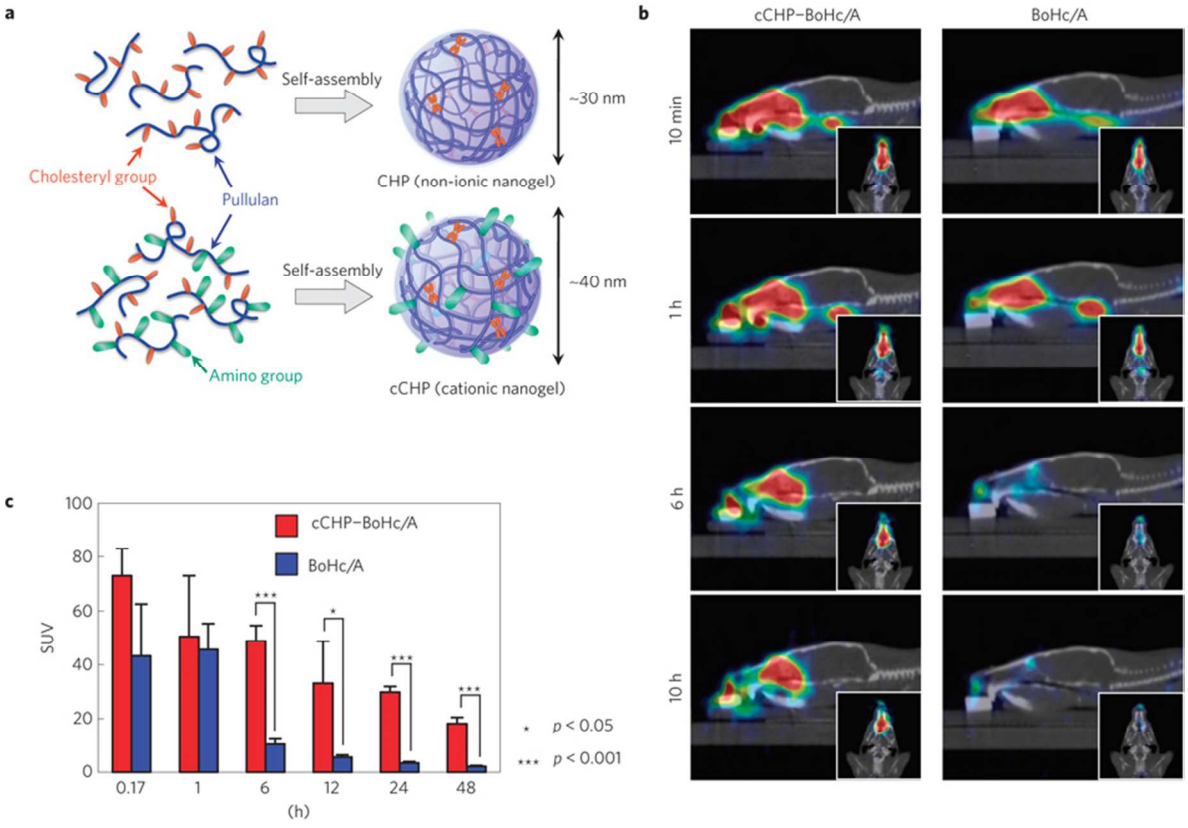


**Figure 11.** (a) Schematic representation of the hybrid nanogels. (b) Computed tomography images of the delivered to the nasal mucosa. (c) Retention of BoHc/A in the nasal tissues after intranasal immunization. Reprinted by permission from Macmillan Publishers Ltd: Nature Materials from Ref. 239, copyright (2010).

Clinical trials of CHP nanogels yielded promising results. In a phase I clinical trial, a CHP-HER2 complex vaccine was administrated to HER2-expressing cancer patients to evaluate the safety and immune response to 146HER2.[240] CHP-HER2 vaccine proved to be safe, well tolerated, and to induced HER2-specific CD8+ and/or CD4+ T-cell immune response. In a phase II clinical trial 146HER2-specific antibody responses following CHP-HER2 vaccination were analyzed.[235] The results indicated that CHP-HER2 induced HER2-specific humoral responses. Moreover, the antibody titers increased over repeated vaccinations, and all reached the plateau levels within nine vaccinations.

Similar results were obtained by Kawabata et al.[234, 241] when they evaluated the safety and the humoral immune responses of CHP-HER2 and CHP-NY-ESO-1 combination vaccines with the immuno-adjuvant OK-432 administered to therapy-refractory esophageal cancer patients.

CHP nanogels have shown encouraging results in clinical trials. However, additional optimization will be necessary for clinical approval.[242]

## 5. Future perspectives and conclusions

We have discussed here various aspects of hybrid nanogels and their applicability in nanomedicine. In recent years, it has been demonstrated that nanotechnology when applied to medicine can provides superior therapeutics and ways to diagnose different diseases. This research area is of such interest that further developments occur almost on a daily basis. The research on multifunctional hybrid nanogels is mostly focused on the synthesis of drug delivery systems due to their ability to efficiently encapsulate therapeutics and release them upon an environmental stimulus. However, the capacity of the hybrid materials to convert external signals to heat, generation of highly oxidative

species, etc., has increased the potential of hybrid nanogels for combinatorial therapies and theranostics.

Furthermore, due to their size and softness, nanogels are easily internalized by the cells and show less accumulation into non-target tissues. Besides these inherent properties of smart nanogels, hybrid nanogels are very attractive because they let new sensitivities to be added to the system via a simple hybridization of the components which allows multiresponsive materials to be obtained. As we have shown in this review, the incorporation of new responsivities to smart nanogels widens the utilization of these systems in several applications such as imaging, guided therapy, and hyperthermia. In this way, it is possible to envision the development of novel materials for nanomedicine that do not only rely on the biological endogenous signals like acidic pH, reductive potential, enzyme overexpression, etc., but also on external stimulus for the triggering of activity. This will enable the preparation of smart nanomaterials with superior targetability and minimized side effects that exert their therapeutic or diagnostic function only at the site where the external trigger was applied.

The hybridization of different kind of material will need to follow a rational screening that ensures the synergistic combination of the best properties of both components toward applications in nanomedicine. This represents a great opportunity for chemists, material scientists, and biologists to develop new methodologies that allow to quickly access to the properties and application potential of newly synthesized hybrid nanogels. In particular, novel biological techniques that provide information about biodegradability, biological fate, and *in vitro* and *in vivo* therapeutic or diagnostic effects upon irradiation, are of great need.

Nevertheless, the application of these new materials in the industry is still in its first steps and there is an urgent need for relevant clinical data relating to safety and efficacy of hybrid nanogels *in vivo*. In particular, a substantial number of unmet issues of the

plasmonic, magnetic, and carbonaceous materials nanoparticles, regarding the pharmacodynamics, metabolism, and pharmacokinetics still need to be assessed before hybrid nanogels can fully make the transition from bench to bedside. We hope that by highlighting the latest and more significant works in the field, we will inspire the community to develop and perform studies toward the clinical use of such promising systems.

## 6. Acknowledgements

We gratefully acknowledge financial support from the Bundesministerium für Bildung und Forschung (BMBF) through the NanoMatFutur award (Thermonanogele, 13N12561), the Helmholtz Virtual Institute, Multifunctional Biomaterials for Medicine, the Freie Universität Focus Area Nanoscale, and the Deutsche Forschungsgemeinschaft (DFG)/German Research Foundation via SFB1112, Project A04. Dr. Maria Molina acknowledges financial support from the Alexander von Humboldt Foundation. Dr. Julian Bergueiro acknowledges financial support from Dahlem Research Center through the Dahlem International Network Postdocs program. We gratefully acknowledge Dr. Pamela Winchester for proofreading the manuscript.

## 7. References

1. M. Hamidi, A. Azadi and P. Rafiei, *Adv. Drug Deliv. Rev.*, 2008, 60, 1638-1649.
2. E. M. Ahmed, *JAR*, 2013, 6, 105-121.
3. Y. Gao, J. Xie, H. Chen, S. Gu, R. Zhao, J. Shao and L. Jia, *Biotechnol. Adv.*, 2014, 32, 761-777.
4. M. Asadian-Birjand, A. Sousa-Herves, D. Steinhilber, J. C. Cuggino and M. Calderon, *Curr. Med. Chem.*, 2012, 19, 5029-5043.
5. A. V. Kabanov and S. V. Vinogradov, *Angew. Chem. Int. Ed.*, 2009, 48, 5418-5429.

6. R. Tong, L. Tang, L. Ma, C. Tu, R. Baumgartner and J. Cheng, *Chem. Soc. Rev.*, 2014, 43, 6982-7012.
7. D. Steinhilber, T. Rossow, S. Wedepohl, F. Paulus, S. Seiffert and R. Haag, *Angew. Chem. Int. Ed.*, 2013, 52, 13538-13543.
8. J. C. Cuggino, C. I. Alvarez I, M. C. Strumia, P. Welker, K. Licha, D. Steinhilber, R.-C. Mutihac and M. Calderon, *Soft Matter*, 2011, 7, 11259-11266.
9. R. Pelton, *Advances in Colloid and Interface Science*, 2000, 85, 1-33.
10. M. Molina, M. Giulbudagian and M. Calderón, *Macromol. Chem. Phys.*, 2014, 215, 2414-2419.
11. M. Giulbudagian, M. Asadian-Birjand, D. Steinhilber, K. Achazi, M. Molina and M. Calderon, *Polym. Chem.*, 2014, 5, 6909-6913.
12. S. Kazakov, M. Kaholek, I. Gazaryan, B. Krasnikov, K. Miller and K. Levon, *J. Phys. Chem. B*, 2006, 110, 15107-15116.
13. X. Zhang, K. Achazi, D. Steinhilber, F. Kratz, J. Dernedde and R. Haag, *J. Control. Release*, 2014, 174, 209-216.
14. L. Zha, B. Banik and F. Alexis, *Soft Matter*, 2011, 7, 5908-5916.
15. S. Nayak and L. A. Lyon, *Angew. Chem. Int. Ed. Engl.*, 2005, 44, 7686-7708.
16. J. Khandare, M. Calderon, N. M. Dagia and R. Haag, *Chem. Soc. Rev.*, 2012, 41, 2824-2848.
17. Y. Chen, X. Zheng, X. Wang, C. Wang, Y. Ding and X. Jiang, *ACS Macro Lett.*, 2013, 3, 74-76.
18. M. C. Coll Ferrer, R. Ferrier, Jr., D. Eckmann and R. Composto, *J. Nanopart. Res.*, 2012, 15, 1-7.
19. W.-H. Chiang, V. T. Ho, H.-H. Chen, W.-C. Huang, Y.-F. Huang, S.-C. Lin, C.-S. Chern and H.-C. Chiu, *Langmuir*, 2013, 29, 6434-6443.
20. T. M. Ruhland, P. M. Reichstein, A. P. Majewski, A. Walther and A. H. E. Müller, *J. Colloid Interface Sci.*, 2012, 374, 45-53.
21. J.-M. Shen, X.-M. Guan, X.-Y. Liu, J.-F. Lan, T. Cheng and H.-X. Zhang, *Bioconjugate Chem.*, 2012, 23, 1010-1021.
22. H. Wang, F. Ke, A. Mararenko, Z. Wei, P. Banerjee and S. Zhou, *Nanoscale*, 2014, 6, 7443-7452.
23. R. M. Sankar, K. M. Seeni Meera, D. Samanta, P. Jithendra, A. B. Mandal and S. N. Jaisankar, *Colloids Surf., B*, 2013, 112, 120-127.
24. R. M. Sankar, K. M. S. Meera, D. Samanta, A. Murali, P. Jithendra, A. Baran Mandal and S. N. Jaisankar, *R. Soc. Chem. Adv.*, 2012, 2, 12424-12430.
25. M. Look, E. Stern, Q. A. Wang, L. D. DiPlacido, M. Kashgarian, J. Craft and T. M. Fahmy, *J. Clin. Invest.*, 2013, 123, 1741-1749.
26. S. Kim, D. J. Lee, D. S. Kwag, U. Y. Lee, Y. S. Youn and E. S. Lee, *Carbohydr. Polym.*, 2014, 101, 692-698.
27. W. Wu and S. Zhou, in *Nanomaterials in Drug Delivery, Imaging, and Tissue Engineering*, John Wiley & Sons, Inc., 2013, pp. 269-319.
28. J. Ge, E. Neofytou, T. J. Cahill, R. E. Beygui and R. N. Zare, *ACS Nano*, 2011, 6, 227-233.
29. T. Kawano, Y. Niidome, T. Mori, Y. Katayama and T. Niidome, *Bioconjugate Chem.*, 2009, 20, 209-212.
30. W. H. Blackburn, E. B. Dickerson, M. H. Smith, J. F. McDonald and L. A. Lyon, *Bioconjugate Chem.*, 2009, 20, 960-968.
31. X. Liu, H. Guo and L. Zha, *Polym. Int.*, 2012, 61, 1144-1150.
32. A. Lohani, G. Singh, S. S. Bhattacharya and A. Verma, *Journal of Drug Delivery*, 2014, 2014, 11.
33. J. Bergueiro and M. Calderón, *Macromol. Biosci.*, 2014, 15, 183-199.

34. Y. Jiang, J. Chen, C. Deng, E. J. Suuronen and Z. Zhong, *Biomaterials*, 2014, 35, 4969-4985.
35. G. Liu and Z. An, *Polym. Chem.*, 2014, 5, 1559-1565.
36. D. M. Eckmann, R. J. Composto, A. Tsourkas and V. R. Muzykantov, *J. Mater. Chem. B*, 2014, 2, 8085-8097.
37. C. Sanchez, G. J. d. A. A. Soler-Illia, F. Ribot, T. Lalot, C. R. Mayer and V. Cabuil, *Chemistry of Materials*, 2001, 13, 3061-3083.
38. C. Sanchez, B. Julian, P. Belleville and M. Popall, *Journal of Materials Chemistry*, 2005, 15, 3559-3592.
39. W. Wu and S. Zhou, *Nano Rev.*, 2010, 1, 5730.
40. T. Hoare, J. Santamaria, G. F. Goya, S. Irusta, D. Lin, S. Lau, R. Padera, R. Langer and D. S. Kohane, *Nano letters*, 2009, 9, 3651-3657.
41. J. Yang, M.-H. Yao, L. Wen, J.-T. Song, M.-Z. Zhang, Y.-D. Zhao and B. Liu, *Nanoscale*, 2014, 6, 11282-11292.
42. D. Jaque, L. Martinez Maestro, B. Del Rosal, P. Haro-Gonzalez, A. Benayas, J. L. Plaza, E. Martin Rodriguez and J. Garcia Sole, *Nanoscale*, 2014, 6, 9494-9530.
43. V. Shanmugam, S. Selvakumar and C. S. Yeh, *Chem. Soc. Rev.*, 2014, 43, 6254-6287.
44. N. Fomina, J. Sankaranarayanan and A. Almutairi, *Adv. Drug Deliv. Rev.*, 2012, 64, 1005-1020.
45. J. Thevenot, H. Oliveira, O. Sandre and S. Lecommandoux, *Chem. Soc. Rev.*, 2013, 42, 7099-7116.
46. H. Wang, J. Yi, S. Mukherjee, P. Banerjee and S. Zhou, *Nanoscale*, 2014, 6, 13001-13011.
47. R. Liang, M. Wei, D. G. Evans and X. Duan, *Chem. Commun.*, 2014, 50, 14071-14081.
48. X. Lian, J. Jin, J. Tian and H. Zhao, *ACS Appl. Mater. Interfaces*, 2010, 2, 2261-2268.
49. T. Niidome, *Journal of Physics: Conference Series*, 2010, 232, 012011.
50. M. Oishi, H. Hayashi, T. Uno, T. Ishii, M. Iijima and Y. Nagasaki, *Macromol. Chem. Phys.*, 2007, 208, 1176-1182.
51. N. Singh and L. A. Lyon, *Chem. Mater.*, 2007, 19, 719.
52. M. Oishi, T. Nakamura, Y. Jinji, K. Matsuishi and Y. Nagasaki, *J. Mater. Chem.*, 2009, 19, 5909.
53. S. Shi, Q. Wang, T. Wang, S. Ren, Y. Gao and N. Wang, *J. Phys. Chem. B*, 2014, 118, 7177-7186.
54. C. Xiao, S. Chen, L. Zhang, S. Zhou and W. Wu, *Chem. Commun.*, 2012, 48, 11751-11753.
55. D. J. Siegwart, A. Srinivasan, S. A. Bencherif, A. Karunanidhi, J. K. Oh, S. Vaidya, R. Jin, J. O. Hollinger and K. Matyjaszewski, *Biomacromolecules*, 2009, 10, 2300.
56. M. Oishi, A. Tamura, T. Nakamura and Y. Nagasaki, *Adv. Funct. Mater.*, 2009, 19, 827-834.
57. Y. Chen, X. Zheng, X. Wang, C. Wang, Y. Ding and X. Jiang, *ACS Macro Lett.*, 2014, 3, 74-76.
58. T. Nakamura, A. Tamura, H. Murotani, M. Oishi, Y. Jinji, K. Matsuishi and Y. Nagasaki, *Nanoscale*, 2010, 2, 739-746.
59. J. Y. Kim, W. I. Choi, M. Kim and G. Tae, *J. Control. Release*, 2013, 171, 113-121.
60. H. Yasui, R. Takeuchi, M. Nagane, S. Meike, Y. Nakamura, T. Yamamori, Y. Ikenaka, Y. Kon, H. Murotani, M. Oishi, Y. Nagasaki and O. Inanami, *Cancer Lett.*, 2014, 347, 151-158.

61. N. S. Rejinold, R. Ranjusha, A. Balakrishnan, N. Mohammed and R. Jayakumar, *R. Soc. Chem. Adv.*, 2014, 4, 5819.
62. X.-q. Zhao, T.-x. Wang, W. Liu, C.-d. Wang, D. Wang, T. Shang, L.-h. Shen and L. Ren, *J. Mater. Chem.*, 2011, 21, 7240.
63. S. Su, H. Wang, X. Liu, Y. Wu and G. Nie, *Biomaterials*, 2013, 34, 3523-3533.
64. T. Kawano, Y. Niidome, T. Mori, Y. Katayama and T. Niidome, *Bioconjugate Chem.*, 2009, 20, 209-212.
65. Z. Zhang, J. Wang, X. Nie, T. Wen, Y. Ji, X. Wu, Y. Zhao and C. Chen, *J. Am. Chem. Soc.*, 2014, 136, 7317-7326.
66. H. Kang, A. C. Trondoli, G. Zhu, Y. Chen, Y.-J. Chang, H. Liu, Y.-F. Huang, X. Zhang and W. Tan, *ACS Nano*, 2011, 5, 5094.
67. W. Wu, J. Shen, P. Banerjee and S. Zhou, *Biomaterials*, 2011, 32, 598-609.
68. E. V. Panfilova, B. N. Khlebtsov and N. G. Khlebtsov, *Colloid J.*, 2013, 75, 333-338.
69. W. Wu, T. Zhou, A. Berliner, P. Banerjee and S. Zhou, *Chemistry of Materials*, 2010, 22, 1966-1976.
70. W. Wu, N. Mitra, E. C. Y. Yan and S. Zhou, *ACS Nano*, 2010, 4, 4831-4839.
71. J. W. M. Bulte and D. L. Kraitchman, *NMR Biomed.*, 2004, 17, 484-499.
72. C. W. Jung and P. Jacobs, *Magn. Reson. Imaging*, 1995, 13, 661-674.
73. Y.-X. J. Wang, *Quant. Imaging Med. Surg.*, 2011, 1, 35-40.
74. Y.-X. Wang, S. Hussain and G. Krestin, *Eur. Radiol.*, 2001, 11, 2319-2331.
75. G. Shahnaz, C. Kremser, A. Reinisch, A. Vetter, F. Laffleur, D. Rahmat, J. Iqbal, S. Dünnhaupt, W. Salvenmoser, R. Tessadri, U. Griesser and A. Bernkop-Schnürch, *Eur. J. Pharma. Biopharm.*, 2013, 85, 346-355.
76. R. A. M. Heesakkers, G. J. Jager, A. M. Hövels, B. de Hoop, H. C. M. van den Bosch, F. Raat, J. A. Witjes, P. F. A. Mulders, C. H. van der Kaa and J. O. Barentsz, *Radiology*, 2009, 251, 408-414.
77. L. H. Reddy, J. L. Arias, J. Nicolas and P. Couvreur, *Chem. Rev.*, 2012, 112, 5818-5878.
78. X. Wang, Z. Zhou, Z. Wang, Y. Xue, Y. Zeng, J. Gao, L. Zhu, X. Zhang, G. Liu and X. Chen, *Nanoscale*, 2013, 5, 8098-8104.
79. W.-H. Chiang, W.-C. Huang, C.-W. Chang, M.-Y. Shen, Z.-F. Shih, Y.-F. Huang, S.-C. Lin and H.-C. Chiu, *J. Control. Release*, 2013, 168, 280-288.
80. H. K. Patra, N. U. Khaliq, T. Romu, E. Wiechec, M. Borga, A. P. F. Turner and A. Tiwari, *Adv. Healthc. Mater.*, 2014, 3, 526-535.
81. C. Niu, Z. Wang, G. Lu, T. M. Krupka, Y. Sun, Y. You, W. Song, H. Ran, P. Li and Y. Zheng, *Biomaterials*, 2013, 34, 2307-2317.
82. W. Dong, Y. Li, D. Niu, Z. Ma, J. Gu, Y. Chen, W. Zhao, X. Liu, C. Liu and J. Shi, *Adv. Mater.*, 2011, 23, 5392-5397.
83. Y. Wang, F. Xu, C. Zhang, D. Lei, Y. Tang, H. Xu, Z. Zhang, H. Lu, X. Du and G.-Y. Yang, *Nanomedicine : nanotechnology, biology, and medicine*, 2011, 7, 1009-1019.
84. J. H. Hwang, Y.-W. Noh, J.-H. Choi, J.-R. Noh, Y.-H. Kim, G.-T. Gang, K.-S. Kim, H. S. Park, Y. T. Lim, H. Moon, K. S. Hong, H. G. Lee, B. H. Chung and C.-H. Lee, *Magnet. Reson. Med.*, 2014, 71, 1054-1063.
85. J. Lu, S. Ma, J. Sun, C. Xia, C. Liu, Z. Wang, X. Zhao, F. Gao, Q. Gong, B. Song, X. Shuai, H. Ai and Z. Gu, *Biomaterials*, 2009, 30, 2919-2928.
86. S. Srivastava, R. Awasthi, D. Tripathi, M. K. Rai, V. Agarwal, V. Agrawal, N. S. Gajbhiye and R. K. Gupta, *Small*, 2012, 8, 1099-1109.
87. L. Zhu, D. Wang, X. Wei, X. Zhu, J. Li, C. Tu, Y. Su, J. Wu, B. Zhu and D. Yan, *J. Control. Release*, 2013, 169, 228-238.

88. H. Wang, J. Shen, G. Cao, Z. Gai, K. Hong, P. R. Debata, P. Banerjee and S. Zhou, *J. Mater. Chem. B*, 2013, 1, 6225-6234.
89. C.-K. Lim, A. Singh, J. Heo, D. Kim, K. E. Lee, H. Jeon, J. Koh, I.-C. Kwon and S. Kim, *Biomaterials*, 2013, 34, 6846-6852.
90. L. Jiang, Q. Zhou, K. Mu, H. Xie, Y. Zhu, W. Zhu, Y. Zhao, H. Xu and X. Yang, *Biomaterials*, 2013, 34, 7418-7428.
91. A. Soleimani, F. Martinez, V. Economopoulos, P. J. Foster, T. J. Scholl and E. R. Gillies, *J. Mater. Chem. B*, 2013, 1, 1027-1034.
92. H. M. Kim, Y.-W. Noh, H. S. Park, M. Y. Cho, K. S. Hong, H. Lee, D. H. Shin, J. Kang, M.-H. Sung, H. Poo and Y. T. Lim, *Small*, 2012, 8, 666-670.
93. C. Prashant, M. Dipak, C.-T. Yang, K.-H. Chuang, D. Jun and S.-S. Feng, *Biomaterials*, 2010, 31, 5588-5597.
94. J. Liu, C. Detrembleur, A. Debuigne, M.-C. De Pauw-Gillet, S. Mornet, L. Vander Elst, S. Laurent, E. Duguet and C. Jérôme, *J. Mater. Chem. B*, 2014, 2, 1009-1023.
95. W. H. Chiang, V. T. Ho, H. H. Chen, W. C. Huang, Y. F. Huang, S. C. Lin, C. S. Chern and H. C. Chiu, *Langmuir*, 2013, 29, 6434-6443.
96. H. B. Na, I. C. Song and T. Hyeon, *Adv. Mater.*, 2009, 21, 2133-2148.
97. M. H. M. Dias and P. C. Lauterbur, *Magnet. Reson. Med.*, 1986, 3, 328-330.
98. C. Corot, P. Robert, J.-M. Idée and M. Port, *Adv. Drug Deliv. Rev.*, 2006, 58, 1471-1504.
99. J. Pintaske, P. Martirosian, H. Graf, G. Erb, K. P. Lodemann, C. D. Claussen and F. Schick, *Invest. Radiol.*, 2006, 41, 213-221.
100. K. M. L. Taylor, A. Jin and W. Lin, *Angew. Chem. Int. Ed. Engl.*, 2008, 47, 7722-7725.
101. J. Lux, M. Chan, L. Vander Elst, E. Schopf, E. Mahmoud, S. Laurent and A. Almutairi, *J. Mater. Chem. B*, 2013, 1, 6359-6364.
102. M. Bruchez, M. Moronne, P. Gin, S. Weiss and A. P. Alivisatos, *Science*, 1998, 281, 2013-2016.
103. P. Mitchell, *Nature Biotechnol.*, 2001, 19, 1013-1017.
104. I. L. Medintz, H. T. Uyeda, E. R. Goldman and H. Mattoussi, *Nature Mater.*, 2005, 4, 435-446.
105. U. Resch-Genger, M. Grabolle, S. Cavaliere-Jaricot, R. Nitschke and T. Nann, *Nature Meth.*, 2008, 5, 763-775.
106. H. Mattoussi, G. Palui and H. B. Na, *Adv. Drug Deliv. Rev.*, 2012, 64, 138-166.
107. X. Michalet, F. F. Pinaud, L. A. Bentolila, J. M. Tsay, S. Doose, J. J. Li, G. Sundaresan, A. M. Wu, S. S. Gambhir and S. Weiss, *Science*, 2005, 307, 538-544.
108. V. Biju, S. Mundayoor, R. V. Omkumar, A. Anas and M. Ishikawa, *Biotechnol. Adv.*, 2010, 28, 199-213.
109. G. O. Menendez, M. Eva Pichel, C. C. Spagnuolo and E. A. Jares-Erijman, *Photochemical & Photobiological Sciences*, 2013, 12, 236-240.
110. Z. Li, W. Xu, Y. Wang, B. R. Shah, C. Zhang, Y. Chen, Y. Li and B. Li, *Carbohydr. Polym.*, 2015, 121, 477-485.
111. A. P. Alivisatos, *Science*, 1996, 271, 933-937.
112. W. C. W. Chan, D. J. Maxwell, X. Gao, R. E. Bailey, M. Han and S. Nie, *Curr. Opin. Biotech.*, 2002, 13, 40-46.
113. U. Hasegawa, S.-i. M. Nomura, S. C. Kaul, T. Hirano and K. Akiyoshi, *Biochem. Biophys. Res. Commun.*, 2005, 331, 917-921.
114. S. Rejinold N, K. P. Chennazhi, H. Tamura, S. V. Nair and J. Rangasamy, *ACS Appl. Mater. Interfaces*, 2011, 3, 3654-3665.
115. Y.-Q. Wang, Y.-Y. Zhang, F. Zhang and W.-Y. Li, *J. Mater. Chem.*, 2011, 21, 6556-6562.

116. W. Wu, T. Zhou, J. Shen and S. Zhou, *Chem. Commun.*, 2009, 4390-4392.
117. D. Jańczewski, N. Tomczak, M.-Y. Han and G. J. Vancso, *Macromolecules*, 2009, 42, 1801-1804.
118. Z. Cheng, A. Al Zaki, J. Z. Hui, V. R. Muzykantov and A. Tsourkas, *Science*, 2012, 338, 903-910.
119. A. M. Smith, H. Duan, A. M. Mohs and S. Nie, *Adv. Drug Deliv. Rev.*, 2008, 60, 1226-1240.
120. K. Park, S. Lee, E. Kang, K. Kim, K. Choi and I. C. Kwon, *Adv. Funct. Mater.*, 2009, 19, 1553-1566.
121. W. Wu, M. Aiello, T. Zhou, A. Berliner, P. Banerjee and S. Zhou, *Biomaterials*, 2010, 31, 3023-3031.
122. H. Zhu, Y. Li, R. Qiu, L. Shi, W. Wu and S. Zhou, *Biomaterials*, 2012, 33, 3058-3069.
123. W. Wu, J. Shen, P. Banerjee and S. Zhou, *Biomaterials*, 2010, 31, 8371-8381.
124. P. Yang, S. Gai and J. Lin, *Chem. Soc. Rev.*, 2012, 41, 3679-3698.
125. I. I. Slowing, J. L. Vivero-Escoto, B. G. Trewyn and V. S. Y. Lin, *J. Mater. Chem.*, 2010, 20, 7924-7937.
126. Z. Tao, *R. Soc. Chem. Adv.*, 2014, 4, 18961-18980.
127. X. Hu, X. Hao, Y. Wu, J. Zhang, X. Zhang, P. C. Wang, G. Zou and X.-J. Liang, *J. Mater. Chem. B*, 2013, 1, 1109-1118.
128. A. Agostini, L. Mondragón, A. Bernardos, R. Martínez-Máñez, M. D. Marcos, F. Sancenón, J. Soto, A. Costero, C. Manguan-García, R. Perona, M. Moreno-Torres, R. Aparicio-Sanchis and J. R. Murguía, *Angew. Chem. Int. Ed. Engl.*, 2012, 51, 10556-10560.
129. H. Meng, M. Xue, T. Xia, Y.-L. Zhao, F. Tamanoi, J. F. Stoddart, J. I. Zink and A. E. Nel, *J. Am. Chem. Soc.*, 2010, 132, 12690-12697.
130. I. I. Slowing, J. L. Vivero-Escoto, C.-W. Wu and V. S. Y. Lin, *Adv. Drug Deliv. Rev.*, 2008, 60, 1278-1288.
131. I. I. Slowing, B. G. Trewyn, S. Giri and V. S. Y. Lin, *Adv. Funct. Mater.*, 2007, 17, 1225-1236.
132. J. L. Vivero-Escoto, I. I. Slowing, B. G. Trewyn and V. S. Y. Lin, *Small*, 2010, 6, 1952-1967.
133. S. Chai, J. Zhang, T. Yang, J. Yuan and S. Cheng, *Colloids Surf., A*, 2010, 356, 32-39.
134. G. Liu, C. Zhu, J. Xu, Y. Xin, T. Yang, J. Li, L. Shi, Z. Guo and W. Liu, *Colloids Surf., B*, 2013, 111, 7-14.
135. B. Chang, D. Chen, Y. Wang, Y. Chen, Y. Jiao, X. Sha and W. Yang, *Chem. Mater.*, 2013, 25, 574-585.
136. B.-S. Tian and C. Yang, *J. Nanosci. Nanotechnol.*, 2011, 11, 1871-1879.
137. W. Feng, W. Nie, C. He, X. Zhou, L. Chen, K. Qiu, W. Wang and Z. Yin, *ACS Appl. Mater. Interfaces*, 2014, 6, 8447-8460.
138. D. F. Acevedo, J. Balach, C. R. Rivarola, M. C. Miras and C. A. Barbero, *Faraday Discuss.*, 2006, 131, 235-252.
139. J. Balach, H. Wu, F. Polzer, H. Kirmse, Q. Zhao, Z. Wei and J. Yuan, *RSC Advances*, 2013, 3, 7979-7986.
140. S. Jokar, A. Pourjavadi and M. Adeli, *R. Soc. Chem. Adv.*, 2014, 4, 33001-33006.
141. A.-H. Lu, G.-P. Hao, Q. Sun, X.-Q. Zhang and W.-C. Li, *Macromol. Chem. Phys.*, 2012, 213, 1107-1131.
142. M. Boot-Handford, J. C. Abanades, E. Anthony, M. Blunt, S. Brandani, N. Mac Dowell, J. Fernandez, M.-C. Ferrari, R. Gross, J. Hallett, S. Haszeldine, P.

Heptonstall, A. Lyngfelt, Z. Makuch, E. Mangano, M. Pourkashanian, G. Rochelle, N. Shah, J. Yao and P. Fennell, *Energy Environ. Sci.*, 2014, 7, 130-189.
143. Y. Gogotsi and V. Presser, *Carbon nanomaterials*, CRC Press, 2013.
144. J. Gu, S. Su, Y. Li, Q. He and J. Shi, *Chem. Commun.*, 2011, 47, 2101-2103.
145. M. Adeli, R. Soleyman, Z. Beiranvand and F. Madani, *Chem. Soc. Rev.*, 2013, 42, 5231-5256.
146. E. Mehdipoor, M. Adeli, M. Bavadi, P. Sasanpour and B. Rashidian, *Journal of Materials Chemistry*, 2011, 21, 15456-15463.
147. H. W. Kroto, J. R. Heath, S. C. O'Brien, R. F. Curl and R. E. Smalley, *Nature*, 1985, 318, 162-163.
148. S. Bosi, T. Da Ros, G. Spalluto and M. Prato, *Eur. J. Med. Chem.*, 2003, 38, 913-923.
149. Z. Chen, L. Ma, Y. Liu and C. Chen, *Theranostics*, 2012, 2, 238.
150. P. Mroz, Y. Xia, D. Asanuma, A. Konopko, T. Zhiyentayev, Y.-Y. Huang, S. K. Sharma, T. Dai, U. J. Khan, T. Wharton and M. R. Hamblin, *Nanomedicine*, 2011, 7, 965-974.
151. N. Saito, H. Haniu, Y. Usui, K. Aoki, K. Hara, S. Takanashi, M. Shimizu, N. Narita, M. Okamoto, S. Kobayashi, H. Nomura, H. Kato, N. Nishimura, S. Taruta and M. Endo, *Chem. Rev.*, 2014, 114, 6040-6079.
152. E. L. Hopley, S. Salmasi, D. M. Kalaskar and A. M. Seifalian, *Biotechnol. Adv.*, 2014, 32, 1000-1014.
153. C. Barbero, R. Coneo Rodriguez, R. Rivero, M. Martinez, M. Molina, J. Balach, M. Bruno, G. Planes, D. Acevedo, C. Rivarola and M. Miras, in *Aquananotechnology*, CRC Press, 2014, pp. 15-54.
154. R. Bellingeri, F. Alustiza, N. Picco, D. Acevedo, M. A. Molina, R. Rivero, C. Grosso, C. Motta, C. Barbero and A. Vivas, *J. Appl. Polym. Sci.*, 2014, 132, DOI: 10.1002/app.41370.
155. Y. Qin, J. Chen, Y. Bi, X. Xu, H. Zhou, J. Gao, Y. Hu, Y. Zhao and Z. Chai, *Acta Biomater.*, 2015, doi:10.1016/j.actbio.2015.1001.1026.
156. A. K. Geim and K. S. Novoselov, *Nature Mater.*, 2007, 6, 183-191.
157. H. Y. Mao, S. Laurent, W. Chen, O. Akhavan, M. Imani, A. A. Ashkarran and M. Mahmoudi, *Chem. Rev.*, 2013, 113, 3407-3424.
158. K. Yang, L. Feng, X. Shi and Z. Liu, *Chem. Soc. Rev.*, 2013, 42, 530-547.
159. R. Mo, T. Jiang, W. Sun and Z. Gu, *Biomaterials*, 2015, 50, 67-74.
160. J. T. Robinson, S. M. Tabakman, Y. Liang, H. Wang, H. Sanchez Casalongue, D. Vinh and H. Dai, *J. Am. Chem. Soc.*, 2011, 133, 6825-6831.
161. N. Lu, J. Liu, J. Li, Z. Zhang, Y. Weng, B. Yuan, K. Yang and Y. Ma, *J. Mater. Chem. B*, 2014, 2, 3791-3798.
162. Y. Zhang, T. R. Nayak, H. Hong and W. Cai, *Nanoscale*, 2012, 4, 3833-3842.
163. C. Wang, J. Mallela, U. S. Garapati, S. Ravi, V. Chinnasamy, Y. Girard, M. Howell and S. Mohapatra, *Nanomedicine*, 2013, 9, 903-911.
164. A. M. Schrand, S. A. C. Hens and O. A. Shenderova, *Critical Reviews in Solid State and Materials Sciences*, 2009, 34, 18-74.
165. V. N. Mochalin, O. Shenderova, D. Ho and Y. Gogotsi, *Nat. Nanotechnol.*, 2012, 7, 11-23.
166. E. K. Chow, X.-Q. Zhang, M. Chen, R. Lam, E. Robinson, H. Huang, D. Schaffer, E. Osawa, A. Goga and D. Ho, *Science Translational Medicine*, 2011, 3, 73ra21.
167. L. Moore, E. K.-H. Chow, E. Osawa, J. M. Bishop and D. Ho, *Adv. Mater.*, 2013, 25, 3532-3541.
168. H.-J. Kim, K. Zhang, L. Moore and D. Ho, *ACS Nano*, 2014, 8, 2998-3005.
169. Y. Kotsuchibashi and R. Narain, *Polym. Chem.*, 2014, 5, 3061.

170. Z. Wu, X. Zhang, H. Guo, C. Li and D. Yu, *J. Mater. Chem.*, 2012, 22, 22788-22796.
171. J. Fan, X. Jiang, Y. Hu, Y. Si, L. Ding and W. Wu, *Biomater. Sci.*, 2013, 1, 421-433.
172. M. Nic, J. Jirat and B. Kosata, *IUPAC Compendium of Chemical Terminology Gold Book*, 2014.
173. Z. Xing, C. Wang, J. Yan, L. Zhang, L. Li and L. Zha, *Soft Matter*, 2011, 7, 7992-7997.
174. E. S. Dragan, *Chem. Eng. J.*, 2014, 243, 572-590.
175. V. Koul, R. Mohamed, D. Kuckling, H.-J. P. Adler and V. Choudhary, *Colloids Surf., B*, 2011, 83, 204-213.
176. R. C. Mundargi, S. A. Patil, P. V. Kulkarni, N. N. Mallikarjuna and T. M. Aminabhavi, *J. Microencapsul.*, 2008, 25, 228-240.
177. H. Jiang, C. W. Lo and D. Zhu, Google Patents, 2013.
178. Z. Li, J. Shen, H. Ma, X. Lu, M. Shi, N. Li and M. Ye, *Soft Matter*, 2012, 8, 3139-3145.
179. D. Schmaljohann, *Adv. Drug Deliv. Rev.*, 2006, 58, 1655-1670.
180. Y. Chen, D. Ding, Z. Mao, Y. He, Y. Hu, W. Wu and X. Jiang, *Biomacromolecules*, 2008, 9, 2609-2614.
181. N. do Nascimento Marques, P. S. Curti, A. M. da Silva Maia and R. d. C. Balaban, *J. Appl. Polym. Sci.*, 2013, 129, 334-345.
182. T. Zhou, C. Xiao, J. Fan, S. Chen, J. Shen, W. Wu and S. Zhou, *Acta Biomater.*, 2013, 9, 4546-4557.
183. Y. Qiu and K. Park, *Adv. Drug Deliv. Rev.*, 2001, 53, 321-339.
184. V. Ramesh Babu, K. S. V. Krishna Rao, M. Sairam, B. V. K. Naidu, K. M. Hosamani and T. M. Aminabhavi, *J. Appl. Polym. Sci.*, 2006, 99, 2671-2678.
185. X. Liu, X. Wang, L. Zha, D. Lin, J. Yang, J. Zhou and L. Zhang, *Journal of Materials Chemistry C*, 2014, 2, 7326-7335.
186. M. Y. Sha, H. Xu, S. G. Penn and R. Cromer, *Nanomedicine*, 2007, 2, 725-734.
187. J. He, B. Yan, L. Tremblay and Y. Zhao, *Langmuir*, 2011, 27, 436-444.
188. S. Schachschal, A. Balaceanu, C. Melian, D. E. Demco, T. Eckert, W. Richtering and A. Pich, *Macromolecules*, 2010, 43, 4331-4339.
189. C. D. Jones and L. A. Lyon, *Macromolecules*, 2000, 33, 8301-8306.
190. X.-b. Liu, J.-f. Zhou and X.-d. Ye, *Chinese Journal of Chemical Physics*, 2012, 25, 463-468.
191. W. Zhang, R. Yao, W. Tao, H. He and S. Shui, *Colloid Polym. Sci.*, 2013, 292, 317-324.
192. S. Zschoche, J. C. Rueda, M. Binner, H. Komber, A. Janke, K.-F. Arndt, S. Lehmann and B. Voit, *Macromol. Chem. Phys.*, 2012, 213, 215-226.
193. W. He, Y. Lv, Y. Zhao, C. Xu, Z. Jin, C. Qin and L. Yin, *Int. J. Pharm.*, 2015, 484, 163-171.
194. X. Li, P. Du and P. Liu, *R. Soc. Chem. Adv.*, 2014, 4, 56323-56331.
195. S. Nayak, H. Lee, J. Chmielewski and L. A. Lyon, *J. Am. Chem. Soc.*, 2004, 126, 10258-10259.
196. E. Dickerson, W. Blackburn, M. Smith, L. Kapa, L. A. Lyon and J. McDonald, *BMC Cancer*, 2010, 10, 10.
197. C. W. Park, H.-M. Yang, H. J. Lee and J.-D. Kim, *Soft Matter*, 2013, 9, 1781.
198. L. Zhao, C. Xiao, J. Ding, P. He, Z. Tang, X. Pang, X. Zhuang and X. Chen, *Acta Biomater.*, 2013, 9, 6535-6543.
199. T. Xing, B. Lai, X. Ye and L. Yan, *Macromol. Biosci.*, 2011, 11, 962-969.
200. W. Shen, Y. Chang, G. Liu, H. Wang, A. Cao and Z. An, *Macromolecules*, 2011, 44, 2524-2530.

201. G. Tamura, Y. Shinohara, A. Tamura, Y. Sanada, M. Oishi, I. Akiba, Y. Nagasaki, K. Sakurai and Y. Amemiya, *Polym. J.*, 2011, 44, 240-244.
202. K. Knop, R. Hoogenboom, D. Fischer and U. S. Schubert, *Angew. Chem. Int. Ed. Engl.*, 2010, 49, 6288-6308.
203. W. Richtering and A. Pich, *Soft Matter*, 2012, 8, 11423.
204. G. R. Hendrickson, M. H. Smith, A. B. South and L. A. Lyon, *Adv. Funct. Mater.*, 2010, 20, 1697-1712.
205. V. Lapeyre, C. Ancla, B. Catargi and V. Ravaine, *J. Colloid Interface Sci.*, 2008, 327, 316-323.
206. N. Bhuchar, R. Sunasee, K. Ishihara, T. Thundat and R. Narain, *Bioconjugate Chem.*, 2012, 23, 75-83.
207. L. A. Picos-Corrales, A. Licea-Claveríe and K.-F. Arndt, *J. Polym. Sci. A Polym. Chem.*, 2012, 50, 4277-4287.
208. Y. C. Wenqing Shen, Haifang Wang, Guangyao Liu, and Z. A. Aoneng Cao, *J. Control. Release*, 2011, 152, e75-e76.
209. Y. Chen, X. Zheng, H. Qian, Z. Mao, D. Ding and X. Jiang, *ACS Appl. Mater. Interfaces*, 2010, 2, 3532-3538.
210. J. Zhang, F. Yang, H. Shen and D. Wu, *ACS Macro Lett.*, 2012, 1, 1295-1299.
211. Y. S. Goshu Tamura, Isamu Akiba, Atsushi Tamura, Motoi Oishi, Yukio Nagasaki, Kazuo Sakurai, Yoshiyuki Amemiya, *JPCS*, 2011, 272, 012018.
212. M. H. Smith and L. A. Lyon, *Acc. Chem. Res.*, 2012, 45, 985-993.
213. Y. Zhu, J. Shi, W. Shen, X. Dong, J. Feng, M. Ruan and Y. Li, *Angew. Chem. Int. Ed. Engl.*, 2005, 44, 5083-5087.
214. J. Wu, T.-M. Sun, X.-Z. Yang, J. Zhu, X.-J. Du, Y.-D. Yao, M.-H. Xiong, H.-X. Wang, Y.-C. Wang and J. Wang, *Biomater. Sci.*, 2013, 1, 1143-1150.
215. G. Ashwell and J. Harford, *Annu. Rev. Biochem.*, 1982, 51, 531-554.
216. D. Dorwal, *Int. J. Pharm. Pharm. Sci.*, 2012, 4, 8.
217. S. Maya, B. Sarmento, A. Nair, N. S. Rejinold, S. V. Nair and R. Jayakumar, *Curr. Pharm. Des.*, 2013, 19, 7203-7218.
218. G. Soni and K. S. Yadav, *SPJ*, doi:10.1016/j.jsps.2014.1004.1001.
219. M. M. Yallapu, M. Jaggi and S. C. Chauhan, *Drug Discov. Today*, 2011, 16, 457-463.
220. W. Wu and S. Zhou, *Macromol. Biosci.*, 2013, 13, 1464-1477.
221. S. Dasgupta, S. K. Ghosh, S. Ray, S. Singh Kaurav and B. Mazumder, *Curr. Drug Delivery*, 2014, 11, 132-138.
222. P. Somasundaran, S. C. Mehta, L. Rhein and S. Chakraborty, *MRS Bull.*, 2007, 32, 779-786.
223. S. A. Ferreira, F. M. Gama and M. Vilanova, *Nanomedicine*, 2013, 9, 159-173.
224. J. Gilmore, X. Yi, L. Quan and A. Kabanov, *J. Neuroimmune Pharmacol.*, 2008, 3, 83-94.
225. S. V. Vinogradov, *Expert Opin. Drug Deliv.*, 2007, 4, 5-17.
226. S. Vinogradov, E. Batrakova and A. Kabanov, *Colloids Surf., B*, 1999, 16, 291-304.
227. S. V. Vinogradov, E. V. Batrakova and A. V. Kabanov, *Bioconjugate Chem.*, 2003, 15, 50-60.
228. M. C. Coll Ferrer, V. V. Shuvaev, B. J. Zern, R. J. Composto, V. R. Muzykantov and D. M. Eckmann, *PLoS ONE*, 2014, 9, e102329.
229. K. Akiyoshi, S. Yamaguchi and J. Sunamoto, *Chem. Lett.*, 1991, 20, 1263-1266.
230. K. Akiyoshi, S. Deguchi, N. Moriguchi, S. Yamaguchi and J. Sunamoto, *Macromolecules*, 1993, 26, 3062-3068.
231. K. Akiyoshi, I. Taniguchi, H. Fukui and J. Sunamoto, *Eur. J. Pharma. Biopharm.*, 1996, 42, 286-290.

232. K. Akiyoshi, S. Kobayashi, S. Shichibe, D. Mix, M. Baudys, S. Wan Kim and J. Sunamoto, *J. Control. Release*, 1998, 54, 313-320.
233. T. Shimizu, T. Kishida, U. Hasegawa, Y. Ueda, J. Imanishi, H. Yamagishi, K. Akiyoshi, E. Otsuji and O. Mazda, *Biochem. Biophys. Res. Commun.*, 2008, 367, 330-335.
234. A. Uenaka, H. Wada, M. Isobe, T. Saika, K. Tsuji, E. Sato, S. Sato, Y. Noguchi, R. Kawabata, T. Yasuda, Y. Doki, H. Kumon, K. Iwatsuki, H. Shiku, M. Monden, A. A. Jungbluth, G. Ritter, R. Murphy, E. Hoffman, L. J. Old and E. Nakayama, *Cancer Immun.*, 2007, 7, 9.
235. S. Kageyama, S. Kitano, M. Hirayama, Y. Nagata, H. Imai, T. Shiraishi, K. Akiyoshi, A. M. Scott, R. Murphy, E. W. Hoffman, L. J. Old, N. Katayama and H. Shiku, *Cancer Sci.*, 2008, 99, 601-607.
236. Y. Lee, S. Y. Park, C. Kim and T. G. Park, *J. Control. Release*, 2009, 135, 89-95.
237. N. Alles, N. S. Soysa, M. D. A. Hussain, N. Tomomatsu, H. Saito, R. Baron, N. Morimoto, K. Aoki, K. Akiyoshi and K. Ohya, *Eur. J. Pharm. Sci.*, 2009, 37, 83-88.
238. H. F. Staats and K. W. Leong, *Nature Mater.*, 2010, 9, 537-538.
239. T. Nochi, Y. Yuki, H. Takahashi, S.-i. Sawada, M. Mejima, T. Kohda, N. Harada, I. G. Kong, A. Sato, N. Kataoka, D. Tokuhara, S. Kurokawa, Y. Takahashi, H. Tsukada, S. Kozaki, K. Akiyoshi and H. Kiyono, *Nature Mater.*, 2010, 9, 572-578.
240. S. Kitano, S. Kageyama, Y. Nagata, Y. Miyahara, A. Hiasa, H. Naota, S. Okumura, H. Imai, T. Shiraishi, M. Masuya, M. Nishikawa, J. Sunamoto, K. Akiyoshi, T. Kanematsu, A. M. Scott, R. Murphy, E. W. Hoffman, L. J. Old and H. Shiku, *Clin. Cancer Res.*, 2006, 12, 7397-7405.
241. R. Kawabata, H. Wada, M. Isobe, T. Saika, S. Sato, A. Uenaka, H. Miyata, T. Yasuda, Y. Doki, Y. Noguchi, H. Kumon, K. Tsuji, K. Iwatsuki, H. Shiku, G. Ritter, R. Murphy, E. Hoffman, L. J. Old, M. Monden and E. Nakayama, *Int. J. Cancer*, 2007, 120, 2178-2184.
242. M. Amidi, E. Mastrobattista, W. Jiskoot and W. E. Hennink, *Adv. Drug Deliv. Rev.*, 2010, 62, 59-82.